Final Report

CR-123540

NONLINEAR AND ADAPTIVE ESTIMATION TECHNIQUES IN REENTRY

Andrew H. Jazwinski
Samuel Pines
Conrad Hipkins
Paul Flanagan

Report No. 72-6
Contract NAS8-26973

February 1972

ANALYTICAL MECHANICS ASSOCIATES, INC.
10210 GREENBELT ROAD
SEABROOK, MARYLAND 20801

FOREWORD

This report describes work performed under contract NAS8-26973 for the NASA Marshall Space Flight Center. The authors are indebted to Dr. Stephen Winder of NASA/MSFC for the support of this work.

The first author, Mr. Jazwinski, is with Business and Technological Systems, Inc., Bowie, Maryland.

TABLE OF CONTENTS

1.0 INTRODUCTION

The objective of this study is the development and testing by simulation of nonlinear and adaptive estimators for reentry (e.g. space shuttle) navigation and model parameter estimation or identification. Of particular interest is the identification of vehicle lift and drag characteristics in real time, since these are important for guidance and control.

Published work in reentry estimation (Ref. [3]) indicates the importance of nonlinear effects in reentry trajectory estimation. In post flight trajectory reconstruction, batch least squares methods tend to diverge, and the standard Extended Kalman filter appears unsuitable for real time applications. This motivates the application of nonlinear filtering techniques (Ref. [1]) to the reentry problem. Some related work on ballistic reentry trajectory estimation may be found in Ref. [4].

To meet the objectives of the study, several nonlinear filters were developed and simulated. In addition, adaptive filters for the real time identification of vehicle lift and drag characteristics, and unmodelable acceleration, were also developed and tested by simulation. The simulations feature an uncertain system environment with rather arbitrary model errors, thus providing a definitive test of estimator performance.

It was found that nonlinear effects are indeed significant in reentry trajectory estimation and a nonlinear filter is demonstrated which successfully tracks through nonlinearities without degrading the information content of the data. Under the same conditions, the usual Extended Kalman filter diverges and is useless. Interesting relationships are also found between nonlinearities and tracking geometry.

The J-Adaptive filter, developed in the course of this study, is shown to successfully track errors in the modeled vehicle lift and drag characteristics. The same filter concept is also shown to track successfully through rather arbitrary

model errors, including lift and drag errors, vehicle mass errors, atmospheric density errors and wind gusts.

The report is organized as follows: Section 3.0 and 4.0 describe the trajectory and measurement models. The "real" system and system model are described in Section 5.0. Nonlinear and adaptive estimators are developed in general form in Section 6.0 and specialized to the problem at hand in Section 7.0. Section 8.0 presents the various partial derivatives required in the estimator equations. Of particular note is our closed-form (analytic) approximation to the state transition matrix, which is apparently quite successful and efficient. Simulations of the various filters are presented in Section 9.0 and our conclusions and recommendations follow in Section 10.0.

2.0 LIST OF SYMBOLS*

A	Azimuth
$\bar{A}$	Unit vector defined in Eqn. (3-10)
a_1, a_2	Parameters defined in Eqn. (A-13)
(a_x, a_y, a_z)	Components of sensed acceleration vector along e_x, e_y, e_z axes
C_A	Error coefficient in drag model (p. 5-2)
$C_{L\alpha}$	Error coefficient in lift model (p. 5-2)
C_L	Lift coefficient
C_D	Drag coefficient
C_u	Correlation matrix (Eqn. (6-19)
c	Speed of sound
c_2	Constant in Eqn. (7-3)
D	Drag vector
d	Oblateness displacement vector given in Eqn. (3-8)
d_r	Vector in earth equatorial plane, orthogonal to the projection of R onto that plane; defined in Eqn. (3-17)
E	Elevation
e	Eccentricity of earth ellipse
(e_x, e_y, e_z)	Unit vectors defining the inertial (geocentric) rectangular coordinate system; e_z through the north pole, e_x and e_y in equatorial plane, e_x to the Vernal Equinox of epoch.
$(e_{x_t}, e_{y_t}, e_{z_t})$	Unit vectors of topocentric coordinate system; e_{x_t} south, e_{y_t} east, e_{z_t} positive upward along the local vertical

*Symbols for intermediate quantities in the partial derivatives of Section 8.0 are defined there and are not included in this list of symbols.

f	System function
g	Gravitational acceleration vector
GHA	Greenwich hour angle
h	Altitude above oblate earth; measurement function
$\bar{H}$	(Pseudo) unit angular momentum vector define in Eqn. (3-9)
I	Identity matrix
J_2	Earth oblateness coefficient
K	Estimater gain matrix
k_1	Error parameter in density model (p. 5-2)
L	Lift vector
M	Mach number; Matrix of measurement partials
m	Vehicle (constant) mass
N	Matrix of partials defined in Eqn. (6-23)
P	State estimation error covariance matrix
Q	Process noise covariance matrix
R	Vehicle inertial position vector with components (x, y, z); measurement noise covariance matrix
r	Magnitude of R
R'	Vector orthogonal to local geodetic horizon plane, Eqn. (3-7)
R_ρ	Vector from station to vehicle in inertial coordinates
r_ρ	Range (magnitude of R_ρ)
R_s	Station position vector in inertial coordinates

r_o	Radius of oblate earth
r_E	Earth equatorial radius
r_p	Earth polar radius
S	Vehicle reference area
t	Time
U	Covariance matrix of u
u	Model error vector
V	Inertial velocity vector, equals $\dot{R}$
v	Measurement noise vector
V_A	Velocity vector of atmosphere given in Eqn. (3-6)
V_R	Velocity vector of vehicle relative to the atmosphere
(v_ρ, v_A, v_E)	Noise in radar measurement
$(v_{a_x}, v_{a_y}, v_{a_z})$	Noise in acceleration measurement
v_R	Magnitude of V_R
W	Wind velocity vector
w	Process noise vector
w_E	Magnitude of wind velocity to the east
w_N	Magnitude of wind velocity to the north
x	State vector
(x, y, z)	Components of R along the axes (e_x, e_y, e_z)
(x_s, y_s, z_s)	Components of R_s

(x_t, y_t, z_t)	Topocentric coordinates of vehicle
Y	Residual Covariance matrix
y	Measurement vector
y_a	Acceleration measurement vector
y_r	Radar measurement vector
y_{am}	Modeled acceleration measurement
y_{rm}	Modeled radar measurement
α	Angle of attack
β	Roll angle (around relative velocity vector)
Δ	Residual function (Eqn. (6-13))
ϵ, ϵ_a	Vectors defining Q (Eqns. (7-3), (7-4))
η_1, η_2	Error coefficients in drag model (p. 5-2)
η_k	kth iterate (Eqs. (6-8), (6-11))
θ	Longitude
θ_t	Right ascension (see Figure 2)
μ	Universal gravitational constant times the mass of the earth
ξ	Variable in Appendix A
ξ_k	kth iterate (Eqn. (6-11))
ρ	Atmospheric density
$(\sigma_{ax}, \sigma_{ay}, \sigma_{az})$	Standard deviations of acceleration measurement noise
$(\sigma_\rho, \sigma_A, \sigma_E)$	Standard deviations of radar measurement noise

τ	Time interval (Eqn. (8-1))
Φ	State transition matrix
φ	Geocentric latitude
φ_g	Geodetic latitude
ψ	Matrix of partials defined in Eqn. (6-23)
Ω	Earth rotation vector
ω	Magnitude of Ω

Other symbols, subscripts and superscripts:

$(\dot{})$	First time derivative
$(\ddot{})$	Second time derivative
$\lvert . \rvert$	Magnitude of a vector
$(\bar{})$	Unit vector
(i)	Time index
$\frac{\partial ( )}{\partial \xi}$	Partial derivative with respect to ξ
$\mathcal{E}\{\cdot\}$	Expectation operator
$(\hat{})$	Estimate of quantity in parentheses
(i|j)	At time i, given measurements up to time j

Conventions:

All vectors are column vectors; superscript T denotes a vector (matrix) transpose. The vector cross product of the vectors a and b is written a x b.

3.0 TRAJECTORY MODEL

The vehicle translational motion is described in an inertial (geocentric) rectangular coordinate system. The earth is assumed to be oblate and rotating. Forces acting on the vehicle consist of gravity, lift and drag. If R is the vehicle (center of gravity) position vector, then the motion is described by

$$\ddot{R} = g + \frac{L+D}{m} \tag{3-1}$$

It is assumed that vehicle turns are coordinated, so that a sideforce is only produced by a rotation of the lift vector around the relative velocity vector.

It is necessary to describe the accelerations on the right-hand side of Equation (3-1) in our inertial coordinate system. This will be done with the aid of Figure 1. Now the gravitational acceleration g is given by

$$g = -\frac{\mu R}{r^3} + \underbrace{\frac{\mu J_2}{r^5}\left[-1 + 5\left(\frac{z}{r}\right)^2\right]R - \frac{2\mu J_2 z}{r^5} e_z}_{\text{Oblateness}} \tag{3-2}$$

The magnitudes of lift and drag are modeled as

$$|L| = \tfrac{1}{2} \rho v_R^2 S C_L , \tag{3-3}$$

$$|D| = \tfrac{1}{2} \rho v_R^2 S C_D , \tag{3-4}$$

where v_R is the magnitude of the relative velocity vector (relative to the atmosphere),

$$V_R = V - V_A \quad . \tag{3-5}$$

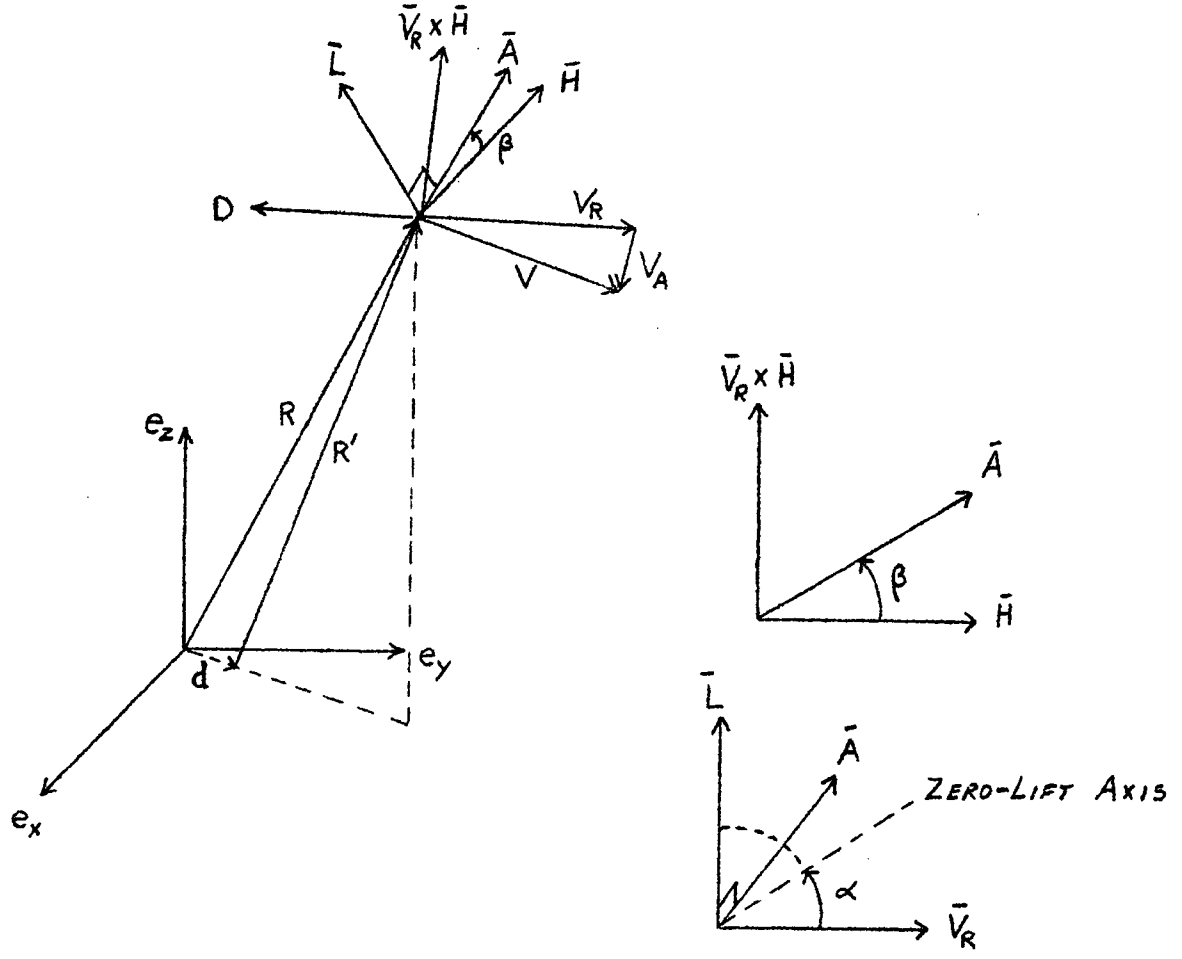

FIGURE 1

Inertial Coordinate System

$V = \dot{R}$ is the inertial velocity vector, and V_A is the velocity of the atmosphere, given by

$$V_A = \Omega x\, R + W. \tag{3-6}$$

Models for atmospheric density ρ, lift and drag coefficients C_L and C_D, and winds W will be described subsequently. First, we determine the inertial directions of L and D.

The vector R', shown in Figure 1, is orthogonal to the local geodetic horizon plane, and is given by

$$R' = R - d \tag{3-7}$$

where

$$d = e^2_x e_x + e^2_y e_y \ . \tag{3-8}$$

(See Appendix A - Figure of the Earth.) Then the unit (pseudo) angular momentum vector

$$\bar{H} = \frac{R' x V_R}{|R' x V_R|} \tag{3-9}$$

is orthogonal to the local horizon and to the relative velocity vector. The roll angle β (roll around relative velocity vector) is measured in the plane defined by $\bar{H}$ and $\bar{V}_R x \bar{H}$. If we define

$$\bar{A} = \cos\beta\, \bar{H} + \sin\beta\ \bar{V}_R \times \bar{H}\ , \tag{3-10}$$

then the lift direction is given by

$$\bar{L} = \bar{V}_R x\, \bar{A}\ . \tag{3-11}$$

The direction of drag is clearly $-\bar{V}_R$.

Now the lift and drag accelerations in Eqn. (3-1) can be written as

$$\frac{L+D}{m} = \frac{1}{2m} \rho S v_R \left[-C_D V_R + C_L V_R \times \bar{A} \right] . \tag{3-12}$$

Our equations of motion, in first order form, are then given by

$$\dot{R} = V ,$$

$$\dot{V} = -\frac{\mu R}{r^3} + \frac{\mu J_2}{r^5} \left[-1 + 5 \left(\frac{z}{r} \right)^2 \right] R - \frac{2\mu J_2 z}{r^5} e_z \tag{3-13}$$

$$+ \frac{1}{2m} \rho S v_R \left[- C_D V_R + C_L V_R \times \bar{A} \right] .$$

We now turn to a description of the atmosphere and vehicle aerodynamics. Atmospheric density is taken as a tabulated function of altitude (see Appendix B), where altitude is given by

$$h = r - r_o, \; r_o = \frac{r_E}{\left\{ 1 + \left[\frac{e^2}{1-e^2} \right] \left(\frac{z}{r} \right)^2 \right\}^{\frac{1}{2}}} , \tag{3-14}$$

The wind velocity vector (in Eqn. (3-6)) is taken of the form

$$W = w_E \frac{e_z \times R}{|e_z \times R|} + w_N \frac{d_r \times R'}{|d_r \times R'|} \tag{3-15}$$

where

$$d_r = y\, e_x - x\, e_y . \tag{3-16}$$

w_E is the wind component blowing to the east, and w_N is the wind component blowing to the north.

The lift and drag coefficients of the vehicle $C_L(\alpha, M)$, $C_D(\alpha, M)$ are taken as tabulated functions of angle of attack α and Mach number M (see Appendix B), where the Mach number is given by

$$M = \frac{v_R}{c} . \tag{3-17}$$

The speed of sound c is taken as a tabulated function of altitude (see Appendix B).

4.0 MEASUREMENT EQUATIONS

Measurements consist of radar tracking and on-board linear accelerations. These are described in the next two subsections.

4.1 Radar Tracking

Radar tracking consists of range, azimuth and elevation measurements. Referring to Figure 2, we see that range r_ρ is given by

$$r_\rho = |R_\rho| \tag{4-1}$$

where

$$R_\rho = R - R_s \ , \tag{4-2}$$

and R_s is the station position vector.

Azimuth and elevation are most easily expressed in the topocentric coordinate system (Figure 2). It is seen that

$$A = \tan^{-1}\left(\frac{y_t}{-x_t}\right) \tag{4-3}$$

and

$$E = \tan^{-1}\frac{z_t}{(r_\rho^2 - z_t^2)^{\frac{1}{2}}} \tag{4-4}$$

Also,

$$\sin A = \frac{y_t}{(r_\rho^2 - z_t^2)^{\frac{1}{2}}} \ , \ \cos A = \frac{-x_t}{(r_\rho^2 - z_t^2)^{\frac{1}{2}}} \ , \ \sin E = \frac{z_t}{r_\rho} \ , \ \cos E = \frac{(r_\rho^2 - z_t^2)^{\frac{1}{2}}}{r_\rho} . \tag{4-5}$$

To express azimuth and elevation in terms of inertial coordinates, we develop the transformation from topocentric coordinates to our inertial frame. The transformation

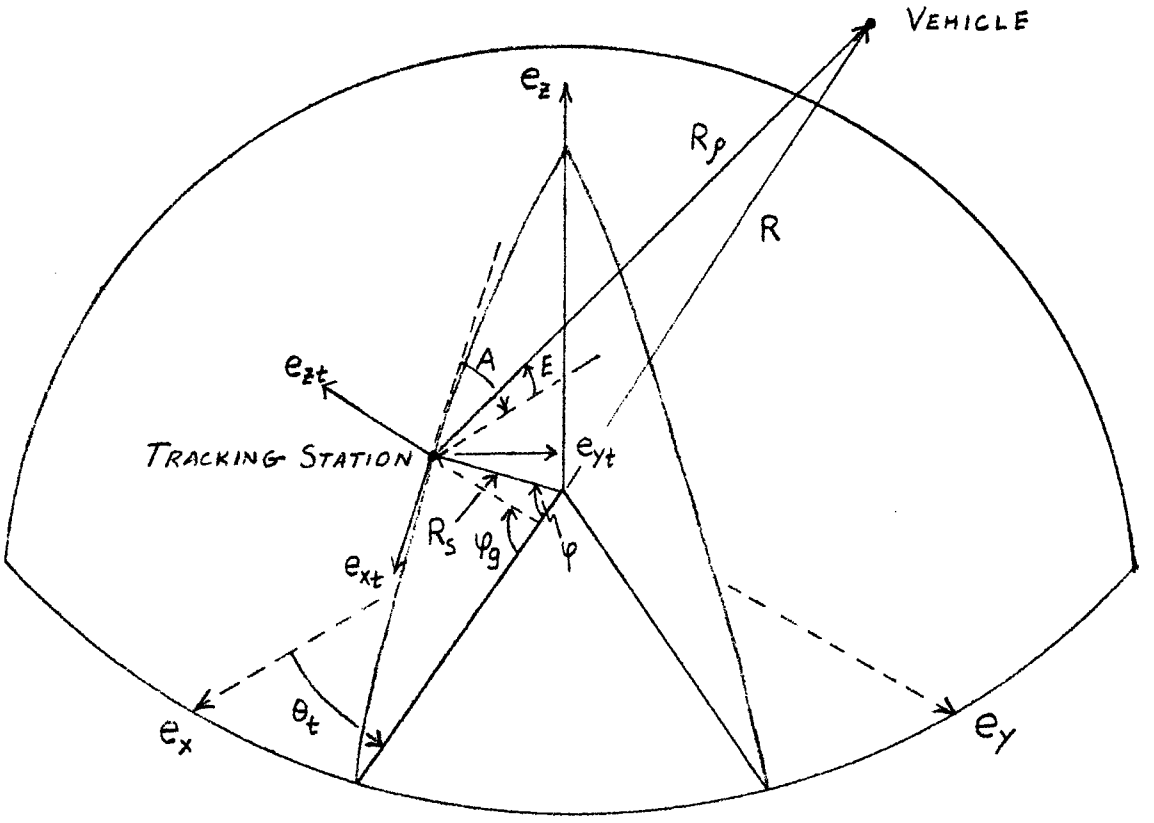

FIGURE 2

Topocentric Coordinate System

$$\begin{bmatrix} \cos\theta_t & \sin\theta_t & 0 \\ -\sin\theta_t & \cos\theta_t & 0 \\ 0 & 0 & 1 \end{bmatrix}$$

rotates (e_x, e_y, e_z) through the angle θ_t around the e_z axis, so that e_x passes through the station meridian. Then the transformation

$$\begin{bmatrix} \sin\varphi_g & 0 & -\cos\varphi_g \\ 0 & 1 & 0 \\ \cos\varphi_g & 0 & \sin\varphi_g \end{bmatrix}$$

brings the resulting frame in coincidence with the topocentric frame. Thus we have

$$\begin{bmatrix} x_t \\ y_t \\ z_t \end{bmatrix} = \begin{bmatrix} \sin\varphi_g\cos\theta_t & \sin\varphi_g\sin\theta_t & -\cos\varphi_g \\ -\sin\theta_t & \cos\theta_t & 0 \\ \cos\varphi_g\cos\theta_t & \cos\varphi_g\sin\theta_t & \sin\varphi_g \end{bmatrix} R_\rho \,. \quad (4\text{-}6)$$

Here, of course, θ_t and φ_g, are the right ascension and geodetic latitude of the station.

It remains to express R_s, the inertial position of the station, in terms of geodetic latitude, longitude and altitude of the station. Aside from a rotation through the angle θ_t, this is given in Eqn. (A-15) of Appendix A. If the earth cross section of Figure A is the station meridian plane, then

$$x_s = \xi \cos\theta_t$$

$$y_s = \xi \sin\theta_t$$

and in view of Eqn. (A-15),

$$x_s = (r_E a_1 + h) \cos \varphi_g \cos \theta_t$$

$$y_s = (r_E a_1 + h) \cos \varphi_g \sin \theta_t \qquad (4\text{-}7)$$

$$z_s = (r_E a_2 + h) \sin \varphi_g$$

(x_s, y_s, z_s) are the components of R_s. Of course,

$$\theta_t = GHA + \theta \qquad (4\text{-}8)$$

where GHA is the Greenwich hour angle and θ the station longitude.

4.2 Linear Accelerations

Accelerations along the inertial (e_x, e_y, e_z) axes are presently considered. These are given by

$$a_x = \left(\frac{L+D}{m}\right)^T e_x, \quad a_y = \left(\frac{L+D}{m}\right)^T e_y \quad , \quad a_z = \left(\frac{L+D}{m}\right)^T e_z \quad , \qquad (4\text{-}9)$$

where (L+D)/m is given in Eqn. (3-12).

5.0 THE DYNAMICAL SYSTEM

Having developed the dynamical equations of motion (3-13) and the measurement equations [(4-1), (4-3), (4-4), (4-9)], we are now in a position to define the dynamical system for estimation. In general, we make a distinction between what we shall call the real system and the system model. Of course, the real system will be a simulated one in the present study. The differences between the two systems are in general shown in Table 1. They consist of different input constants and errors in atmospheric density, winds and C_L and C_D, added to the real system to produce the system model. The real system will be used to generate the measurements which will be processed by estimators designed on the basis of the system model. We shall usually make no notational distinction between the real and model systems.

Real system dynamics are given in Eqs. (3-13). The (real) measurements are given by

$$y_r = \begin{bmatrix} r_{\rho\,(REAL)} \\ A_{(REAL)} \\ E_{(REAL)} \end{bmatrix} + \begin{bmatrix} v_\rho \\ v_A \\ v_E \end{bmatrix}, \tag{5-1}$$

where $r_{\rho\,(REAL)}$, $A_{(REAL)}$, $E_{(REAL)}$ are given by Eqs. (4-1), (4-3) and (4-4), respectively; and by

$$y_a = \begin{bmatrix} a_{x(REAL)} \\ a_{y(REAL)} \\ a_{z(REAL)} \end{bmatrix} + \begin{bmatrix} v_{a_x} \\ v_{a_y} \\ v_{a_z} \end{bmatrix}, \tag{5-2}$$

where $a_{x(REAL)}$, $a_{y(REAL)}$, $a_{z(REAL)}$ are given by Eqs. (4-9). v_ρ, v_A, v_E, v_{a_x}, v_{a_y}, v_{a_z} are independent, zero-mean, white Gaussian noises with respective

REAL SYSTEM	SYSTEM MODEL
J_2 REAL	J_2 MODEL
m REAL	m MODEL
ρ REAL	ρ MODEL = ρ REAL $(1 + k_1)$
w_E, w_N REAL	w_E, w_N MODEL = w_E, w_N REAL $+ \Delta w_E$, Δw_N
C_L REAL	C_L MODEL = C_L REAL + $C_{L\alpha}$ α
C_D REAL	C_D MODEL = C_D REAL + C_A $+ \eta_1 \alpha + \eta_2 \alpha^2$

k_1, $C_{L\alpha}$, C_A, η_1, η_2 ~ constants

TABLE 1

REAL AND MODEL SYSTEMS

standard deviations σ_ρ, σ_A, σ_E, σ_{a_x}, σ_{a_y}, σ_{a_z}. Measurements are sampled at discrete time instants t_i, so that at time t_i an estimator will process

$$y_r(i), \quad y_a(i). \tag{5-3}$$

Estimators are designed on the basis of the system model. We always estimate the position R and velocity V of the vehicle. To this end we define the 6-dimensional state vector x,

$$x^T = \left[x_1 \; x_2 \; x_3 \; \vdots \; x_4 \; x_5 \; x_6 \right] = \left[R^T \; \vdots \; V^T \right]. \tag{5-4}$$

Sometimes we estimate errors in the lift and drag coefficients ΔC_L and ΔC_D. In that case we can define the 2-vector

$$u = \begin{bmatrix} \Delta C_L \\ \Delta C_D \end{bmatrix} \tag{5-5}$$

and modify the dynamical Equations (3-13) by replacing C_L by

$$C_L + u_1 \tag{5-6}$$

and C_D by

$$C_D + u_2. \tag{5-7}$$

We also make these replacements in the accelerations of Eqs. (4-9). When we estimate unknown (or unmodeled) accelerations we define a 3-vector u to represent these unknown accelerations. In this case u is added to the right-hand side of the second of Equations (3-13), and to the accelerations in Eqs. (4-9).

Let $f(\cdot)$ be the six-vector mapping defined by Equations (3-13), with the system model parameters as given in Table 1. Then the system dynamical model is given by

$$x(i+1) = f(x(i), \; u(i)) \; + \; w(i) \tag{5-8}$$

where u is either a 2-vector of C_L and C_D errors (Eq. (5-5)), or a 3-vector of unknown accelerations. w is a 6 x 1 vector of independent, zero-mean, white Gaussian noises. Both u and w will be made specific in connection with each estimation algorithm.

Measurements are modeled as

$$y_{rm}(i) = h^1(x(i)) + v^1(i) \quad , \tag{5-9}$$

$$y_{am}(i) = h^2(x(i),\ u(i)) + v^2(i) \quad , \tag{5-10}$$

where

$$h^1(x(i)) = \begin{bmatrix} r_\rho(x(i)) \\ A(x(i)) \\ E(x(i)) \end{bmatrix} \quad , \quad h^2(x(i),\ u(i)) = \begin{bmatrix} a_x(x(i),\ u(i)) \\ a_y(x(i),\ u(i)) \\ a_z(x(i),\ u(i)) \end{bmatrix}$$

$$v^1(i) = \begin{bmatrix} v_\rho(i) \\ v_A(i) \\ v_E(i) \end{bmatrix} \quad , \quad v^2(i) = \begin{bmatrix} v_{a_x}(i) \\ v_{a_y}(i) \\ v_{a_z}(i) \end{bmatrix} \tag{5-11}$$

To summarize, the real system generates measurements (5-1) and (5-2). Estimators which will process these measurements are based on the model given in Eqs. (5-8), (5-9) and (5-10).

6.0 NONLINEAR AND ADAPTIVE ESTIMATORS

Several nonlinear and adaptive estimators are presented in this section. These estimators will be applied, in Section 7.0, to the present reentry problem. Nonlinear estimators include the Extended Kalman Filter and two local iterations which improve the reference trajectory, and thus the estimate, in the presence of significant nonlinearities. These nonlinear estimation algorithms are discussed in detail in Ref. [1], Chapter 8, Section 3. Adaptive estimators aim, in one instance, at estimating errors in the lift and drag coefficients. In the presence of other, unknown, model errors, the adaptive estimator is designed to track the unknown accelerations.

The basic system model for the nonlinear estimators is given by

$$x(i+1) = f\,(x(i)) + w\,(i)$$

$$y(i) = h\,(x(i)) + v\,(i) \qquad (6\text{-}1)$$

where x is the state vector and y the measurement vector. $\{w(i)\}$, $\{v(i)\}$ are independent, zero-mean white Gaussian noise sequences with

$$\mathcal{E}\,\{w(i)\,w^{T}(i)\} = Q\,(i)$$

$$\mathcal{E}\,\{v(i)\,v^{T}(i)\} = R\,(i) \qquad (6\text{-}2)$$

Estimators involve recursions for the estimate of the state ($\hat{x}$) and the estimation error covariance matrix (P). $\hat{x}(i\,|j)$ is the estimate of the state at time t_i, and $P(i\,|j)$ is the estimation error covariance matrix at time t_i, given all measurements up to and including time t_j.

A basic model for an adaptive estimator is of the form

$$x(i+1) = f\,(x(i),\ u(i)) + w\,(i)$$
$$y(i) = h\,(x(i),\ u(i)) + v\,(i) \qquad (6\text{-}3)$$

Here, u is a random (unknown) forcing function to be estimated.

6.1 Extended Kalman Filter

The Extended Kalman Filter [Ref. [1], p. 278] is the result of applying the (linear) Kalman filter to a linearized nonlinear system which is relinearized about each new estimate of the state as new estimates become available. The result for the system of Eqn. (6-1) is

$$\hat{x}(i+1\,|\,i) = f\,(\hat{x}(i\,|\,i))$$
$$P(i+1\,|\,i) = \Phi\,(i+1,\,i)\ P(i\,|\,i)\ \Phi^{T}(i+1,\,i) + Q\,(i) \qquad (6\text{-}4)$$

$$\hat{x}(i\,|\,i) = \hat{x}\,(i\,|\,i\text{-}1) + K(i)\ [y(i) - h(\hat{x}(i\,|\,i\text{-}1))]$$
$$P(i\,|\,i) = [I - K\,(i)\ M\,(i)]\ P\,(i\,|\,i\text{-}1) \qquad (6\text{-}5)$$

where

$$K(i) = P(i\,|\,i\text{-}1)\ M^{T}(i)\ [M(i)\ P\,(i\,|\,i\text{-}1)\ M^{T}(i) + R(i)]^{-1} \qquad (6\text{-}6)$$

and

$$\Phi\,(i+1,\,i) = \left.\frac{\partial x(i+1)}{\partial x\,(i)}\right|_{\hat{x}(i\,|\,i)}$$
$$M(i) = \left.\frac{\partial h}{\partial x}\right|_{\hat{x}(i\,|\,i\text{-}1)} \qquad (6\text{-}7)$$

Eqs. (6-4) are sometimes called the prediction equations, and Eqs. (6-5) the filter or

update equations.

It is important to note that the state transition matrix Φ and the measurement partials M are evaluated at the current best estimate. Thus they implicitly depend on the estimate. As a consequence of this, the filter gain K also implicitly depends on the estimate.

6.2 Iterated Extended Kalman Filter

The Extended Kalman Filter can be iterated at each measurement to improve the reference trajectory and thus also the estimate [Ref. [1], p. 279]. The iteration involves only the estimate update equation, the first of Eqs. (6-5). That equation is replaced by the iteration

$$\eta_{k+1} = \hat{x}\,(i\,|\,i-1) + K(i,\ \eta_k)\left[y(i) - h(\eta_k) - M(i,\ \eta_k)(\hat{x}(i\,|\,i-1) - \eta_k)\right] \qquad (6\text{-}8)$$

$$k = 1,\ \ldots,\ \ell$$

The iteration starts with

$$\eta_1 = \hat{x}\,(i\,|\,i-1)\ , \qquad (6\text{-}9)$$

and we set

$$\hat{x}(i\,|\,i) = \eta_\ell\ . \qquad (6\text{-}10)$$

Observe that the gain K, matrix M and function h are recomputed each iteration. The covariance matrix $P(i\,|\,i)$ in Eqn. (6-5) is computed only after the iteration has converged. Note that the second iterate, η_2, is merely the output of the Extended Kalman filter.

This iteration has a probabilistic (maximum likelihood) interpretation, which may be found in Ref. [1], Chapter 9, Section 7.

6.3 Iterated Linear Filter - Smoother

The Iterated Extended Kalman Filter is designed for measurement nonlinearities and does not improve the previous reference trajectory on the interval $[t_{i-1}, t_i)$. The latter reference trajectory can be improved by including a smoother (from t_i to t_{i-1}) in the iteration loop, and thus dealing explicitly with dynamical nonlinearities as well. The result is the iterated linear filter-smoother, which also has a maximum likelihood interpretation [Ref. [1], Chapter 9, Section 7].

Given $\hat{x}(i-1|i-1)$ and $P(i-1|i-1)$, the iteration is given by

$$\eta_{k+1} = \hat{x}(i|i-1; \xi_k) + K(i, \eta_k, \xi_k)\, \Delta(i, \eta_k, \xi_k)$$

$$\xi_{k+1} = \hat{x}(i-1|i-1) + P(i-1|i-1)\, \Phi^T(i, i-1; \xi_k)\, M^T(i, \eta_k) Y^{-1}(i, \eta_k, \xi_k) \Delta(i, \eta_k, \xi_k) \tag{6-11}$$

$$k = 1, \ldots, \ell$$

where

$$\eta_1 = \hat{x}(i|i-1; \xi_1) \quad , \quad \xi_1 = \hat{x}(i-1|i-1) \tag{6-12}$$

and

$$\hat{x}(i|i-1; \xi_k) = f(\xi_k) + \Phi(i, i-1; \xi_k)\, [\hat{x}(i-1|i-1) - \xi_k]$$

$$P(i|i-1; \xi_k) = \Phi(i, i-1; \xi_k)\, P(i-1|i-1)\, \Phi^T(i, i-1; \xi_k) + Q(i) \tag{6-13}$$

$$\Delta(i, \eta_k, \xi_k) = y(i) - h(\eta_k) - M(i, \eta_k)[\hat{x}(i|i-1; \xi_k) - \eta_k]$$

$$K(i, \eta_k, \xi_k) = P(i|i-1; \xi_k)\, M^T(i, \eta_k)\, Y^{-1}(i, \eta_k, \xi_k)$$

$$Y(i, \eta_k, \xi_k) = M(i, \eta_k)\, P(i|i\text{-}1;\xi_k)\, M^T(i, \eta_k) + R\ (i)$$

At the end of the iteration,

$$\hat{x}(i|i\text{-}1) = \hat{x}\ (i|i\text{-}1;\xi_\ell)$$

$$P(i|i\text{-}1) = P(i|i\text{-}1;\xi_\ell) \qquad (6\text{-}14)$$

and

$$\hat{x}(i|i) = \eta_\ell$$

$$P(i|i) = [I - K(i, \eta_\ell, \xi_\ell)\, M(i, \eta_\ell)]\, P(i|i\text{-}1) \qquad (6\text{-}15)$$

6.4 J-Adaptive Filter

This filter, based on the model in Eqn. (6-3), is designed to track the random forcing function u(i) while estimating the state x(i) via an Extended Kalman filter. Since the dynamics of u are supposed unknown, we assume that

$$u(i+1) = u(i). \qquad (6\text{-}16)$$

In order to track unpredictable variations in u, we maintain the uncertainty in u constant, or some specified function which does not decrease as a result of the estimation process. That is,

$$\mathcal{E}\{[u(i) - \hat{u}(i|j)]\,[u(i) - \hat{u}(i|j)]^T\} = U\ , \qquad (6\text{-}17)$$

where the covariance matrix U is specified.

The J-adaptive filter is derived by augmenting the state x with u, writing the augmented filter in partitioned form, and discarding the equations for the covariance matrix U. This exercise is given in Ref. [1], pp. 281-286. To write the

result, we need, in addition to the state estimation error covariance matrix $P(i|j)$,

$$P(i|j) = \mathcal{E}\{[x(i) - \hat{x}(i|j)]\,[x(i) - \hat{x}(i|j)]^T\} \quad , \tag{6-18}$$

the following correlation matrix

$$C_u(i|j) = \mathcal{E}\{[x(i) - \hat{x}(i|j)]\,[u(i) - \hat{u}(i|j)]^T\} \quad . \tag{6-19}$$

The J-adaptive filter is then given by

$$\begin{aligned}
&\hat{x}(i+1|i) = f(\hat{x}(i|i),\ \hat{u}(i|i)) \quad , \\
&\hat{u}(i+1|i) = \hat{u}(i|i) \quad , \\
&P(i+1|i) = \Phi(i+1,\ i)\,P(i|i)\,\Phi^T(i+1,\ i) + \Phi(i+1,i)\,C_u(i|i)\,\psi^T(i+1,i) \\
&\qquad + \psi(i+1,i)\,C_u^T(i|i)\,\Phi^T(i+1,i) + \psi(i+1,i)\,U\,\psi^T(i+1,i) \\
&\qquad + Q(i) \\
&C_u(i+1|i) = \Phi(i+1,i)\,C_u(i|i) + \psi(i+1,i)\,U,\ C_u(0|0) = 0 \quad ,
\end{aligned} \tag{6-20}$$

$$\begin{aligned}
&\hat{x}(i|i) = \hat{x}(i|i-1) + K_x(i)\,[y(i) - h(\hat{x}(i|i-1),\ \hat{u}(i|i-1))] \quad , \\
&\hat{u}(i|i) = \hat{u}(i|i-1) + K_u(i)\,[y(i) - h(\hat{x}(i|i-1),\ \hat{u}(i|i-1))] \quad , \\
&P(i|i) = P(i|i-1) - K_x(i)\,[M(i)\,P(i|i-1) + N(i)\,C_u^T(i|i-1)] \quad , \\
&C_u(i|i) = C_u(i|i-1) - K_x(i)\,[M(i)\,C_u(i|i-1) + N(i)\,U] \quad ,
\end{aligned} \tag{6-21}$$

where

$$K_x(i) = [P(i|i-1)\, M^T(i) + C_u(i|i-1)\, N^T(i)]\, Y^{-1}(i) \quad ,$$

$$K_u(i) = [C_u{}^T(i|i-1)\, M^T(i) + U\, N^T(i)]\, Y^{-1}(i), \tag{6-22}$$

$$Y(i) = M(i)\, P(i|i-1)\, M^T(i) + M(i)\, C_u(i|i-1)\, N^T(i) + N(i) C_u{}^T(i|i-1) M^T(i)$$

$$+ N(i)\, U\, N^T(i) + R(i)$$

and

$$\Phi(i+1, i) = \frac{\partial x(i+1)}{\partial x(i)} \Bigg|_{\hat{x}(i|i),\ \hat{u}(i|i)} , \quad \psi(i+1, i) = \frac{\partial x(i+1)}{\partial u(i)} \Bigg|_{\hat{x}(i|i),\ \hat{u}(i|i)}$$

$$M(i) = \frac{\partial h}{\partial x} \Bigg|_{\hat{x}(i|i-1),\ \hat{u}(i|i-1)} , \quad N(i) = \frac{\partial h}{\partial u} \Bigg|_{\hat{x}(i|i-1),\ \hat{u}(i|i-1)} \tag{6-23}$$

6.5 Schmidt-Kalman or Consider Filter

This filter (see Ref. [1], p. 285) takes the uncertainties in the vector u into account, but does not track variations in u itself. That is, it assumes that

$$\hat{u}(i|i) = \hat{u}(o) \quad , \tag{6-24}$$

where $\hat{u}(o)$ is the a-priori estimate of u. The Consider filter is obtained from the J-Adaptive filter by throwing away the second of Eqs. (6-21) and replacing it by Eqn. (6-24).

7.0 ESTIMATORS APPLIED TO REENTRY

In order to specialize the estimators described in Section 6.0 to the present reentry problem, we specify the matrices appearing in the estimator equations. These are the matrices of partial derivatives for which the detailed expressions may be found in Section 8.0.

7.1 Extended Kalman and Iterated Filters (Sections 6.1, 6.2, 6.3)

The state transition matrix Φ appearing in Eqs. (6-4), (6-7), (6-11) and (6-13) is the 6 x 6 matrix

$$\Phi(i+1,\ i) = \begin{bmatrix} \dfrac{\partial R_{i+1}}{\partial R_i} & \dfrac{\partial R_{i+1}}{\partial V_i} \\ \\ \dfrac{\partial V_{i+1}}{\partial R_i} & \dfrac{\partial V_{i+1}}{\partial V_i} \end{bmatrix}. \tag{7-1}$$

The system noise covariance matrix Q appearing in Eqs. (6-4) and (6-13) is modeled as the 6 x 6 diagonal matrix

$$Q(i) = \begin{bmatrix} \epsilon_1^{\,2}(i) & & 0 \\ & \ddots & \\ 0 & & \epsilon_6^{\,2}(i) \end{bmatrix}, \tag{7-2}$$

where the 6 x 1 vector $\epsilon(i)$ is defined as

$$\epsilon(i) = c_2 \begin{bmatrix} \dfrac{\tau^2}{2} & \epsilon_a \\ \\ \tau & \epsilon_a \end{bmatrix} \tag{7-3}$$

with c_2 a constant and the 3 x 1 vector ϵ_a defined as

$$\epsilon_a = \frac{L+D}{m} \quad . \tag{7-4}$$

For processing radar measurements, we have the 3 x 6 measurement partials matrix M and the 3 x 3 measurement noise covariance matrix R (in Eqs. (6-5), (6-6), (6-7), (6-8), (6-11) and (6-13))

$$M(i) = \begin{bmatrix} \left[\frac{\partial r_\rho}{\partial R}\right]^T & \vdots & \\ \left[\frac{\partial A}{\partial R}\right]^T & \vdots & \begin{matrix} 3 \times 3 \\ 0 \end{matrix} \\ \left[\frac{\partial E}{\partial R}\right]^T & \vdots & \end{bmatrix} , \quad R(i) = \begin{bmatrix} \sigma_\rho^2 & & 0 \\ & \sigma_A^2 & \\ 0 & & \sigma_E^2 \end{bmatrix} , \tag{7-5}$$

while for acceleration measurements,

$$M(i) = \left[A_r^e \ , \ A_v^e\right], \quad R(i) = \begin{bmatrix} \sigma_{a_x}^2 & & 0 \\ & \sigma_{a_y}^2 & \\ 0 & & \sigma_{a_z}^2 \end{bmatrix} . \tag{7-6}$$

7.2 J-Adaptive Filter for Lift and Drag Coefficients

In the J-Adaptive filter for errors in the lift and drag coefficients, the vector u is the 2-vector defined in Eq. (5-5). The matrices Φ, M and R are as defined in Section 7.1. In addition (see Section 6.4),

$$\psi(i+1,\ i) = \begin{bmatrix} \dfrac{\partial R_{i+1}}{\partial C_L} & \dfrac{\partial R_{i+1}}{\partial C_D} \\ \dfrac{\partial V_{i+1}}{\partial C_L} & \dfrac{\partial V_{i+1}}{\partial C_D} \end{bmatrix} . \tag{7-7}$$

In case of radar measurements,

$$N(i) = \underset{3 \times 2}{0} , \tag{7-8}$$

while for acceleration measurements N is 3 x 2 given by

$$N(i) = \left[A^{e}_{C_L} \ , \ A^{e}_{C_D} \right] . \tag{7-9}$$

The matrix U is a 2 x 2 diagonal matrix with elements u_{ii} which are specified by input.

7.3 J-Adaptive Filter for Unmodeled Accelerations

In the J-Adaptive filter for unmodeled accelerations, the vector u is 3 x 1. The state transition matrix Φ is as given in Eqn. (7-1), while ψ is 6 x 3 given by

$$\psi(i+1,\ i) = \begin{bmatrix} \dfrac{\tau^2}{2} & \underset{3x3}{I} \\ \tau & \underset{3x3}{I} \end{bmatrix} . \tag{7-10}$$

The matrices M and R are as defined in Section 7.1. In case of radar measurements,

$$N(i) = \overset{3x3}{0} \quad , \tag{7-11}$$

while for acceleration measurements N is a 3 x 3 identity matrix. (The latter reflects the fact that sensed acceleration equals modeled acceleration plus u in our model.) The matrix U is a 3 x 3 diagonal matrix with elements u_{ii} which are specified by input.

8.0 PARTIAL DERIVATIVES

The estimators described in the preceding sections require various partial derivatives of the system function and measurement function for their implementation. These derivatives are developed in the following subsections.

8.1 State Transition Matrix

In order to obtain rapidly computable, closed form expressions for the state transition matrix, we make the following approximation (see Ref. [2]). We assume that over short time intervals

$$\tau = t_{i+1} - t_i \quad , \tag{8-1}$$

the accelerations on the vehicle are constant. That is, the right hand side of Eqs. (3-13) are constant. Under this assumption, Eqs. (3-13) can be integrated in closed form to give

$$R_{i+1} = R_i + V_i \tau - \left(\frac{\mu R_i}{r_i^3}\right)\frac{\tau^2}{2} + \left\{\frac{\mu J_2}{r_i^5}\left[-1+5\left(\frac{z_i}{r_i}\right)^2\right]R_i - \frac{2\mu J_2 z_i}{r_i^5} e_z\right\}\frac{\tau^2}{2}$$

$$+ \frac{1}{2m}\rho S v_R\left[-C_D V_R + C_L V_R \times \bar{A}\right]\frac{\tau^2}{2} \quad ,$$

(8-2)

$$V_{i+1} = V_i - \left(\frac{\mu R_i}{r_i^3}\right)\tau + \left\{\frac{\mu J_2}{r_i^5}\left[-1+5\left(\frac{z_i}{r_i}\right)^2\right]R_i - \frac{2\mu J_2 z_i}{r_i^5} e_z\right\}\tau$$

$$+ \frac{1}{2m}\rho S v_R\left[-C_D V_R + C_L V_R \times \bar{A}\right]\tau$$

Eqs. (8-2) are closed form expressions for R_{i+1} and V_{i+1} (at time t_{i+1}) in terms of R_i, V_i, C_D and C_L (at time t_i). We may now obtain the required partials directly by differentiating these expressions. Neglecting the subscript i on the right hand sides of Eqs. (8-2), we obtain

$$\frac{\partial R_{i+1}}{\partial R_i} = I + \frac{\tau^2}{2}\,(G_0 + G_1 + A_r^e)$$

$$\frac{\partial R_{i+1}}{\partial V_i} = \tau\, I + \frac{\tau^2}{2}\, A_V^e$$

$$\frac{\partial R_{i+1}}{\partial C_D} = \frac{\tau^2}{2}\, A_{C_D}^e$$

$$\frac{\partial R_{i+1}}{\partial C_L} = \frac{\tau^2}{2}\, A_{C_L}^e \qquad (8\text{-}3)$$

$$\frac{\partial V_{i+1}}{\partial R_i} = \tau\,(G_0 + G_1 + A_r^e)$$

$$\frac{\partial V_{i+1}}{\partial V_i} = I + \tau\, A_V^e$$

$$\frac{\partial V_{i+1}}{\partial C_D} = \tau\, A_{C_D}^e$$

$$\frac{\partial V_{i+1}}{\partial C_L} = \tau A_{C_L}^e$$

where

$$G_0 = \frac{\mu}{r^3}\left[\frac{3}{r^2}\,RR^T - I\right]$$

$$G_1 = \frac{\mu J_2}{r^5}\left\{\left[-1+5\left(\frac{z}{r}\right)^2\right]I + \frac{5}{r^2}\left[1-7\left(\frac{z}{r}\right)^2\right]RR^T + \frac{10z}{r^2}\left[Re_z^T + (Re_z^T)^T\right] - 2\,e_z e_z^T\right\}$$

$$A_r^e = \frac{S}{2m}\left\{\left[-C_D V_R + C_L V_R x\bar{A}\right]\left[\frac{\partial\rho}{\partial R}v_R + \rho\frac{\partial v_R}{\partial R}\right]^T + \rho v_R\left[-V_R\left(\frac{\partial C_D}{\partial R}\right)^T + \left(V_R x\bar{A}\right)\left(\frac{\partial C_L}{\partial R}\right)^T - C_D\frac{\partial V_R}{\partial R} + C_L\frac{\partial(V_R x\bar{A})}{\partial R}\right]\right\} \tag{8-4}$$

$$A_V^e = \frac{1}{2m}\rho S\left\{\frac{1}{v_R}\left[-C_D V_R + C_L V_R x\bar{A}\right]V_R^T + v_R\left[-V_R\left(\frac{\partial C_D}{\partial V}\right)^T + \left(V_R x\bar{A}\right)\left(\frac{\partial C_L}{\partial V}\right)^T - C_D I + C_L\frac{\partial(V_R x\bar{A})}{\partial V}\right]\right\}$$

$$A_{C_D}^e = -\frac{1}{2m}\rho S v_R V_R$$

$$A_{C_L}^e = \frac{1}{2m}\rho S v_R V_R x\bar{A}$$

and where

$$\frac{\partial\rho}{\partial R} = \frac{\partial\rho}{\partial h}\left(\frac{R}{r} - \frac{\partial r_o}{\partial R}\right)$$

$$\frac{\partial r_o}{\partial R} = \frac{r_o^3 e^2 z}{r_E^2 (1-e^2) r^2} \left(\frac{z}{r^2} R - e_z \right)$$

$$\left(\frac{\partial v_R}{\partial R} \right)^T = \frac{1}{v_R} V_R^T \frac{\partial V_R}{\partial R} = \bar{V}_R^T \frac{\partial V_R}{\partial R}$$

$$\frac{\partial V_R}{\partial R} = \mathcal{L}_1 (\Omega) - \frac{\partial W}{\partial R}$$

$$\mathcal{L}_1(\xi) = \begin{bmatrix} 0 & \xi_z & -\xi_y \\ -\xi_z & 0 & \xi_x \\ \xi_y & -\xi_x & 0 \end{bmatrix} \quad ; \quad \mathcal{L}_2 (\xi) = \frac{1}{|\xi|} \left[I - \bar{\xi} \bar{\xi}^T \right]$$

$$\frac{\partial W}{\partial R} = - w_E \mathcal{L}_2 (e_z \times R) \mathcal{L}_1 (e_z) + w_N \mathcal{L}_2 (d_r \times R') \left[\mathcal{L}_1 (R') \mathcal{L}_1 (e_z) - \mathcal{L}_1 (d_r) \frac{\partial R'}{\partial R} \right]$$

$$\frac{\partial R'}{\partial R} = \begin{bmatrix} (1-e^2) & 0 & 0 \\ 0 & (1-e^2) & 0 \\ 0 & 0 & 1 \end{bmatrix}$$

(8-5)

$$\frac{\partial C_D}{\partial R} = \frac{1}{c} \frac{\partial C_D}{\partial M} \left[\frac{\partial v_R}{\partial R} - \frac{v_R}{c} \frac{\partial c}{\partial h} \left(\frac{R}{r} - \frac{\partial r_o}{\partial R} \right) \right]$$

$$\frac{\partial C_L}{\partial R} = \frac{1}{c} \frac{\partial C_L}{\partial M} \left[\frac{\partial v_R}{\partial R} - \frac{v_R}{c} \frac{\partial c}{\partial h} \left(\frac{R}{r} - \frac{\partial r_o}{\partial R} \right) \right]$$

$$\frac{\partial (V_R \times \bar{A})}{\partial R} = \mathcal{L}_1 (\bar{A}) \frac{\partial V_R}{\partial R} - \mathcal{L}_1 (V_R) \frac{\partial \bar{A}}{\partial R}$$

$$\frac{\partial \bar{A}}{\partial R} = \cos\beta \frac{\partial \bar{H}}{\partial R} + \sin\beta \left[\mathcal{L}_1(\bar{H}) \frac{\partial \bar{V}_R}{\partial R} - \mathcal{L}_1(\bar{V}_R) \frac{\partial \bar{H}}{\partial R} \right]$$

$$\frac{\partial \bar{V}_R}{\partial R} = \mathcal{L}_2(V_R) \frac{\partial V_R}{\partial R}$$

$$\frac{\partial \bar{H}}{\partial R} = \mathcal{L}_2(R' \times V_R) \left[\mathcal{L}_1(V_R) \frac{\partial R'}{\partial R} - \mathcal{L}_1(R') \frac{\partial V_R}{\partial R} \right]$$

$$\frac{\partial C_D}{\partial V} = \frac{1}{c v_R} \frac{\partial C_D}{\partial M} V_R$$

$$\frac{\partial C_L}{\partial V} = \frac{1}{c v_R} \frac{\partial C_L}{\partial M} V_R$$

$$\frac{\partial (V_R \times \bar{A})}{\partial V} = \mathcal{L}_1(\bar{A}) - \mathcal{L}_1(V_R) \frac{\partial \bar{A}}{\partial V}$$

$$\frac{\partial \bar{A}}{\partial V} = -\cos\beta \mathcal{L}_2(R' \times V_R) \mathcal{L}_1(R') + \sin\beta \left[\mathcal{L}_1(\bar{H}) \mathcal{L}_2(V_R) + \mathcal{L}_1(\bar{V}_R) \mathcal{L}_2(R' \times V_R) \mathcal{L}_1(R') \right]$$

These partial derivatives are evaluated at

$$R = \frac{R_{i+1} + R_i}{2} \quad , \quad V = \frac{V_{i+1} + V_i}{2} \qquad (8\text{-}6)$$

$$\alpha = \frac{\alpha_{i+1} + \alpha_i}{2} \quad , \quad \beta = \frac{\beta_{i+1} + \beta_i}{2}$$

8.2 Measurement (First) Partials

The first partial derivatives of the measurements (Section 4.0) are given by

$$\frac{\partial r_\rho}{\partial R} = \frac{R_\rho}{r_\rho}$$

$$\frac{\partial A}{\partial R} = \frac{1}{(r_\rho^2 - z_t^2)} \begin{bmatrix} x_t \sin\theta_t + y_t \cos\theta_t \sin\varphi_g \\ -x_t \cos\theta_t + y_t \sin\theta_t \sin\varphi_g \\ -y_t \cos\varphi_g \end{bmatrix} \tag{8-7}$$

$$\frac{\partial E}{\partial R} = \frac{1}{(r_\rho^2 - z_t^2)^{\frac{1}{2}}} \begin{bmatrix} \cos\theta_t \cos\varphi_g - (z_t/r_\rho^2)(x - x_s) \\ \sin\theta_t \cos\varphi_g - (z_t/r_\rho^2)(y - y_s) \\ \sin\varphi_g - (z_t/r_\rho^2)(z - z_s) \end{bmatrix}$$

and

$$\begin{bmatrix} \left(\frac{\partial a_x}{\partial R}\right)^T \\ \left(\frac{\partial a_y}{\partial R}\right)^T \\ \left(\frac{\partial a_z}{\partial R}\right)^T \end{bmatrix} = \begin{bmatrix} \frac{\partial a_x}{\partial x} & \frac{\partial a_x}{\partial y} & \frac{\partial a_x}{\partial z} \\ \frac{\partial a_y}{\partial x} & \frac{\partial a_y}{\partial y} & \frac{\partial a_y}{\partial z} \\ \frac{\partial a_z}{\partial x} & \frac{\partial a_z}{\partial y} & \frac{\partial a_z}{\partial z} \end{bmatrix} = A_r^e \tag{8-8}$$

$$\begin{bmatrix} \left(\frac{\partial a_x}{\partial V}\right)^T \\ \left(\frac{\partial a_y}{\partial V}\right)^T \\ \left(\frac{\partial a_z}{\partial V}\right)^T \end{bmatrix} = A^e_V \quad ; \quad \begin{bmatrix} \frac{\partial a_x}{\partial C_D} \\ \frac{\partial a_y}{\partial C_D} \\ \frac{\partial a_z}{\partial C_D} \end{bmatrix} = A^e_{C_D} \quad ; \quad \begin{bmatrix} \frac{\partial a_x}{\partial C_L} \\ \frac{\partial a_y}{\partial C_L} \\ \frac{\partial a_z}{\partial C_L} \end{bmatrix} = A^e_{C_L}$$

9.0 SIMULATIONS

This section presents the results of simulations of the various filters described in sections 6.0 and 7.0. Basically, three types of simulations were performed. The first type deals strictly with nonlinearities; that is, a perfect model is assumed. The object here is to study nonlinear effect in the reentry problem. The second type of simulation performed deals with the problem of the identification of time-varying errors in the lift and drag coefficients. Finally, various model errors (see Section 5.0) are introduced and simulations are performed of estimators capable of tracking under such conditions.

All simulations are performed with a diagonal initial covariance matrix (P_0), with a standard deviation of 3 km in the position components, and 150 m/sec in the velocity components. Actual errors in the initial position and velocity estimate are consistent with these statistics. These initial errors are sizeable, but probably realistic at spacecraft acquisition.

Radar tracking is simulated from several tracking stations. During radar coverage a 3-vector measurement of range, azimuth, and elevation is processed every 4 seconds. The noise standard deviations in these measurements are

$$\sigma_\rho = 3\text{m}$$

$$\sigma_A = 0.01^\circ$$

$$\sigma_E = 0.01^\circ$$

When simulated, accelerations are processed as a 3-vector measurement every 4 seconds. The noise standard deviations in these measurements are

$$\sigma_{a_x} = 0.002a_x + 10^{-6} \quad (km/sec^2)$$

$$\sigma_{a_y} = 0.002a_y + 10^{-6} \quad (km/sec^2)$$

$$\sigma_{a_z} = 0.002a_z + 10^{-6} \quad (km/sec^2)$$

9.1 Estimation in the Presence of Nonlinearities

Various simulations of the Extended Kalman, Iterated Extended Kalman and Iterated Linear Filter-Smoother estimators were performed in a perfect model environment with no process noise ($Q \equiv 0$ in the filters). Under certain conditions dramatic nonlinear effects are observed.

Figures 3 and 4 show the time histories of position and velocity errors ($|R-\hat{R}|$ and $|V-\hat{V}|$) for the Extended Kalman and the Iterated Extended Kalman filters during a pass over the first tracking station. This simulation involves tracking only--acceleration measurements appear to have insignificant effect on these results. A family of curves is presented, depending on the line of sight elevation angle (E_o) at spacecraft acquisition (acquisition angle). It is seen that the Extended Kalman filter diverges for high acquisition angles while the Iterated Extended Kalman filter performs well. At low acquisition angles both filters perform similarly and well. The fact that the estimates are generally better after 65 seconds for lower acquisition angles is due to longer duration of radar coverage, as indicated in the figures.

These results have the following interpretation. At high acquisition angles information rates and nonlinearities are high, calling for relatively large corrections. The Extended Kalman filter, designed for linear or nearly linear systems, when called upon to make large corrections, fails and is useless. We apparently have a filter (the Iterated Extended Kalman) capable of tracking under these conditions.

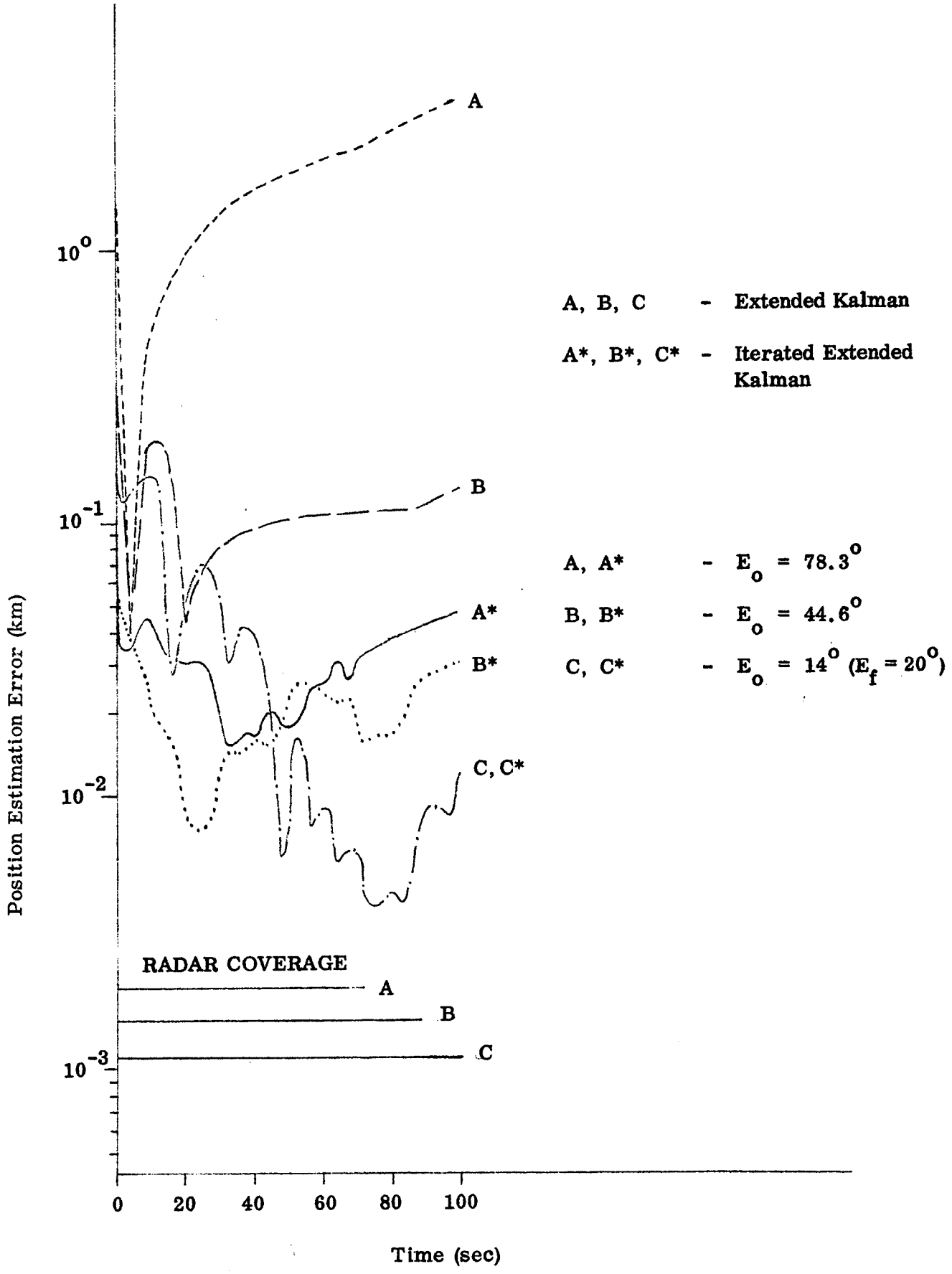

FIGURE 3

Position Estimation Errors

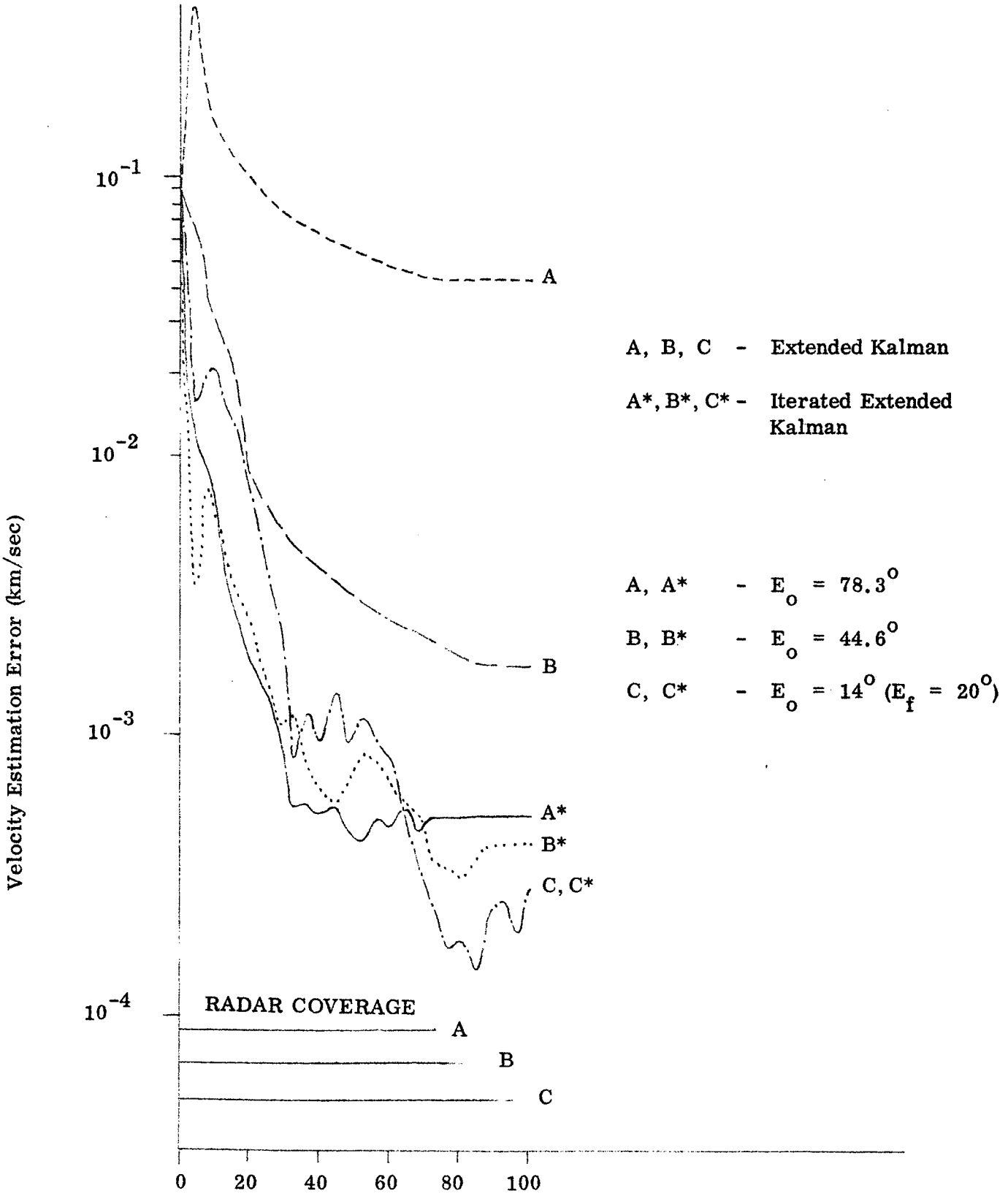

FIGURE 4

Velocity Estimation Errors

At low acquisition angles information rates are low, calling for smaller corrections, and under these conditions the Extended Kalman filter works well. It is to be noted that the covariance matrix of the Iterated Extended Kalman filter is consistent with its estimation errors, while for the Extended Kalman filter it is not. In the latter case errors are orders of magnitude larger than those predicted by the covariance matrix.

An interesting and very significant feature of these results is the fact that the covariance matrices associated with the two filters are the same--to almost two significant digits. This means that linearized error analyses produce good results for the present problem--but, such error analyses are indicative of the performance of an optimal filter, not of the standard Extended Kalman filter. To put it another way, if one has in mind the usual filter, linearized error analysis is wrong, misleading and optimistic. If one has in mind an optimal filter, the error analysis is correct. Our simulations indicate that, in the present case, we have such an optimal filter.

To summarize briefly, these results have significant implications for

(1) filter design,

(2) tracking station (or beacon) placement and tracking schedule design, and

(3) error analyses interpretations,

for reentry trajectory estimation.

It is to be noted that the nonlinear effects seen in Figures 3 and 4 can only be observed during transients when position and velocity uncertainties are relatively high (e.g. acquisition). When Extended Kalman filter C (Figures 3 and 4) encounters the next tracking station at a high acquisition angle, then, provided its errors are low, its performance will be satisfactory. Whether or not its errors will be low at the next station acquisition depends on the length of the data gap. It pays to iterate when uncertainties and information rates are both high. Once uncertainties are brought down, the iteration can be stopped. After approximately 30 seconds, the iteration in filter A* is unnecessary.

Now the divergence of filters A and B (Figures 3 and 4) can be avoided by adding Q to the filter. While divergence can thus be avoided, such a filter will clearly have poorer performance than the Iterated Filter since the system model is then more uncertain. Similar comments apply to the artifice of increasing the measurement noise covariance matrix R - a device sometimes successfully used to prevent filter divergence. The Iterated Extended Kalman filter directly addresses and solves the problem of nonlinearities in the present situation.

The Iterated Linear Filter-Smoother was simulated under various conditions, including high acquisition angles as in Figures 3 and 4. Its performance was generally insignificantly better than that of the Iterated Extended Kalman filter. This is in general agreement with the results obtained by Mehra for ballistic reentry (Ref [4]). System nonlinearities appear less significant than measurement nonlinearities. Now system nonlinearities depend on τ, the time gap between data. For sufficiently large time gaps ($\tau \cong 100$ sec), the Iterated Filter-Smoother shows some improvement over the Iterated Extended Kalman filter, but the latter results were inconsistent. This may perhaps be due to the linearization in the smoothing loop which could perhaps be avoided. This is a possible future research area.

9.2 Identification of C_L and C_D

One of the more important problem areas in atmospheric trajectory estimation is the lack of precise knowledge of the dynamical model. Thus it may be necessary to estimate in real-time certain model parameters, and it can be expected that these parameters or parameter errors will be time-varying. Such estimation is important not only for the trajectory estimation or navigation, but also for guidance and control, which can depend on such parameters. In particular, the model for lift and drag coefficients of the vehicle can be uncertain and, for guidance and control purposes, it may be necessary to estimate such errors in real time.

Errors in the lift and drag models were simulated by setting $C_{L\alpha} = 0.07$, $C_A = 0$, $\eta_1 = -0.05$, $\eta_2 = 0$ (see Table 1, p. 5-2). The resulting errors represent approximately 10% of the real lift and drag coefficients. Figure 5 shows the performance of the J-Adaptive filter for lift and drag coefficients in estimating these lift and drag errors. The simulated error and its estimate via the J-Adaptive filter is plotted. The filter was simulated with $u_{11} = (1.0 \times 10^{-2})^2$ and $u_{22} = (6.0 \times 10^{-3})^2$; $Q \equiv 0$. Tracking and on-board accelerations were used in this simulation.

It is seen in Figure 5 that the J-Adaptive filter tracks these errors extremely well. The error remaining after the estimation is always less than 5% of the simulated error or less than 0.5% of the real lift and drag coefficients; and usually substantially less than this. It should be noted that the filter is not very sensitive to the choice of the matrix U.

Figures 6 and 7 show the resulting position and velocity errors of the J-Adaptive filter. Also shown is the radar coverage (nine traveling stations). Fine detail of the error structure is not shown in these figures. The peaks in the error curves are associated with two phenomena; skips in the reentry trajectory and/or low elevation angle radar coverage or total tracking data gaps. The large peak around 1000 sec corresponds to both a skip and a data gap. Where multiple station coverage is available (e.g. times greater than 1500 sec), estimation errors are brought down to the tracking noise level. It may be noted that the on-board accelerations do not substantially improve the estimation when tracking is available. However, during tracking data gaps, on-board acceleration are very useful in inhibiting further error growth. That is to say, the error peaks during gaps are higher without on-board acceleration data.

The dashed curves in Figures 6 and 7 show the errors for the Consider filter for C_L and C_D; i.e. when C_L and C_D errors are not estimated. Where the dashed curve is absent, the Consider filter errors are similar to the J-Adaptive filter

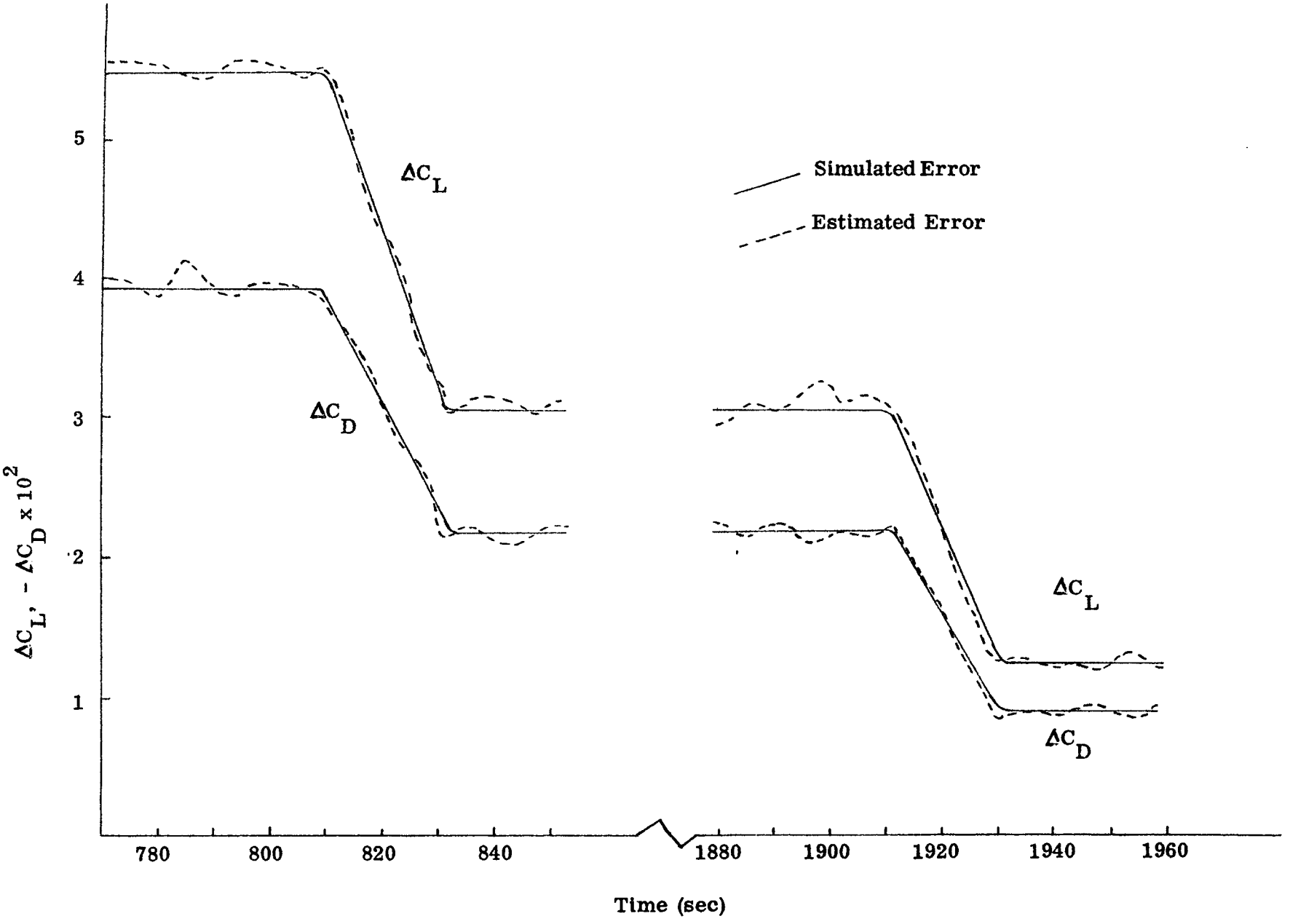

FIGURE 5

Estimation of Lift and Drag Errors

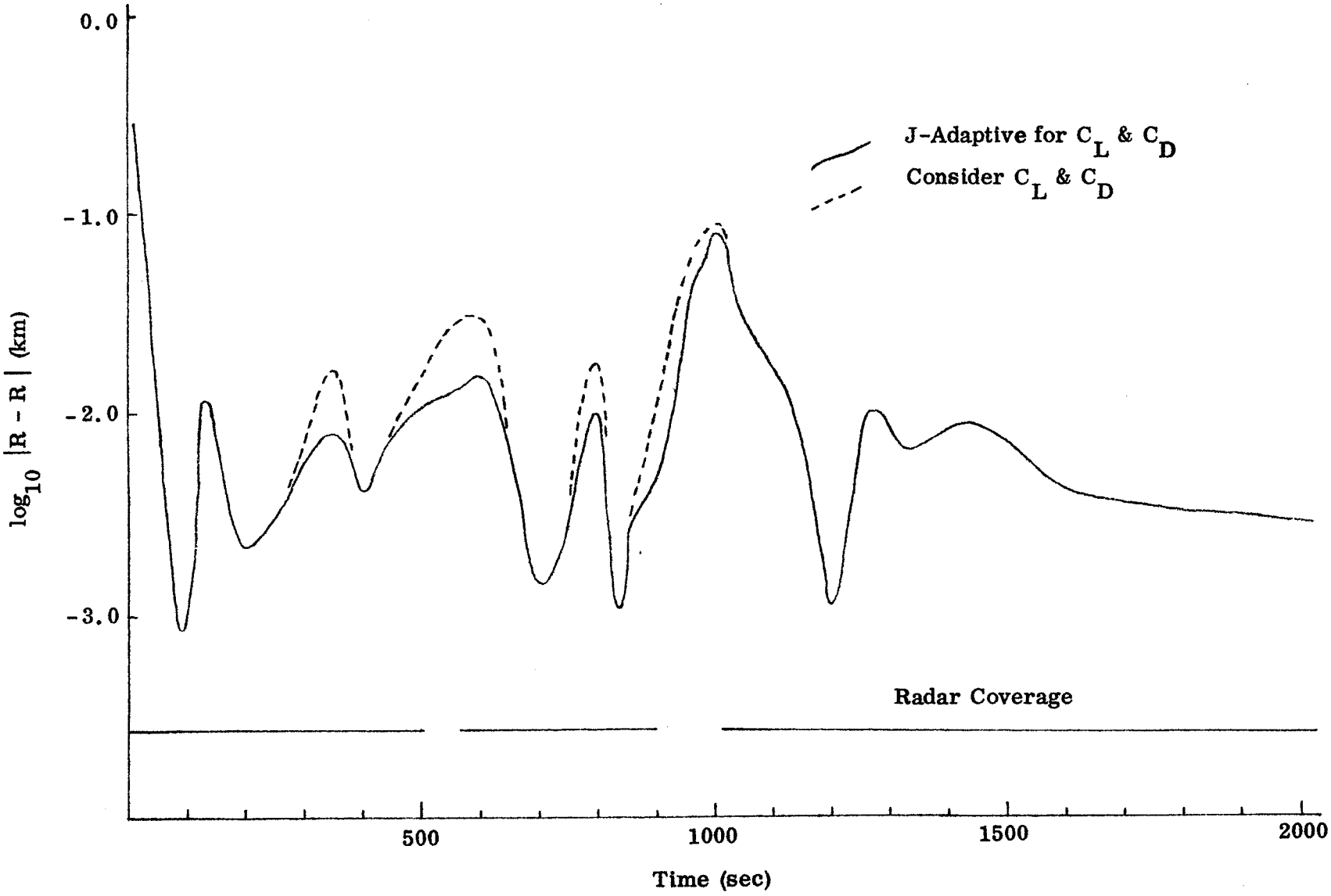

FIGURE 6

Position Estimation Errors

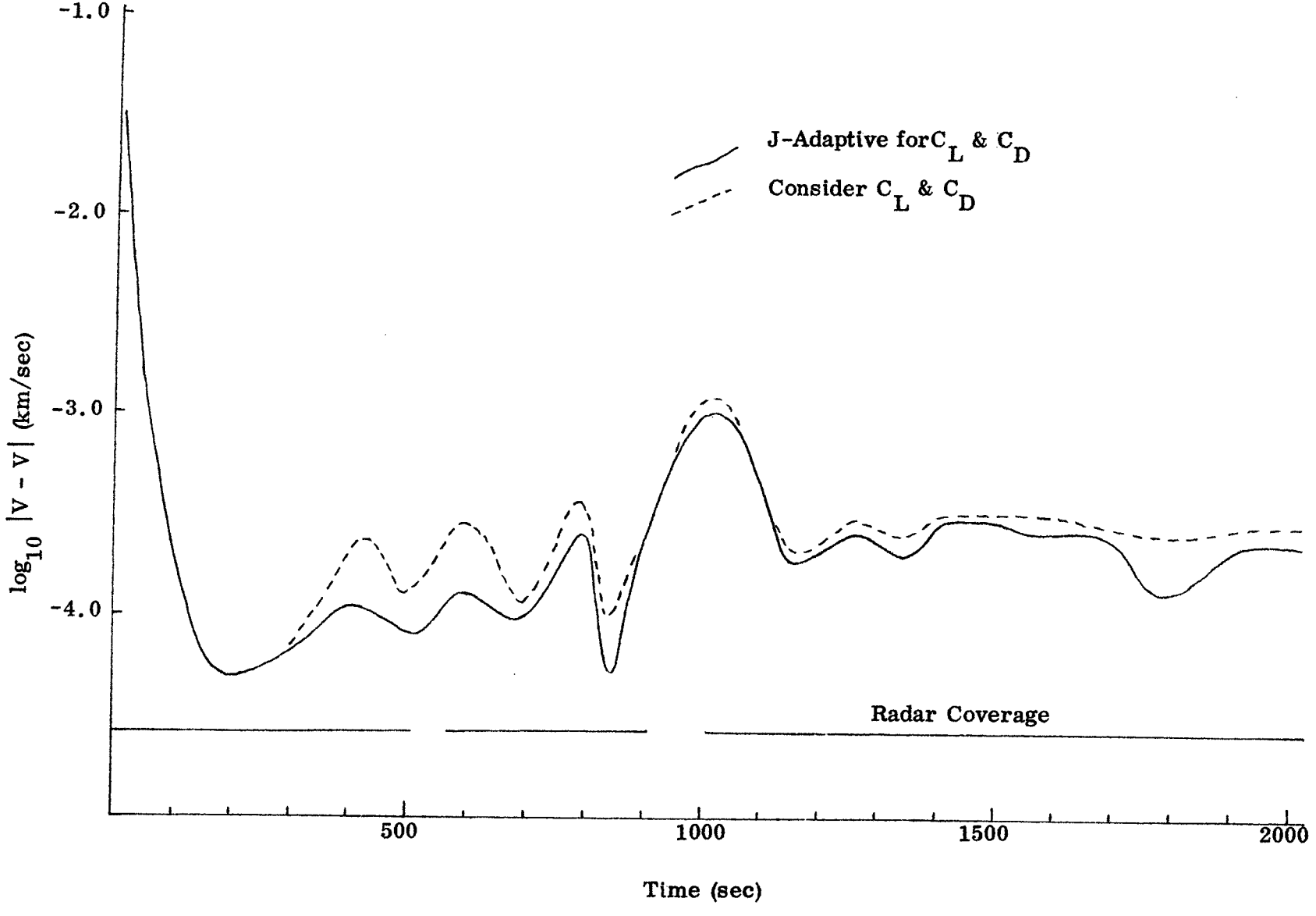

FIGURE 7

Velocity Estimation Errors

errors. The Consider filter performs surprisingly well, despite the fact that C_L and C_D errors are not estimated. Its performance deteriorates somewhat during tracking data gaps when a good model is needed for prediction. The J-Adaptive filter produces a better prediction model than the Consider filter.

9.3 Estimation in the Presence of Arbitrary Model Errors

Several filters are simulated in the presence of arbitrary or unmodelable errors. The errors simulated include the 10% C_L and C_D errors described in Section 9.2. In addition, errors in vehicle mass, atmospheric density and unmodeled winds are simulated. With reference to Table 1 (p.5-2), m REAL = 111448 kg, while m MODEL = 112562 kg. This represents a 1% error in vehicle mass. Density errors are simulated with $k_1 = 0.03$. This represents a 3% error in atmospheric density. The simulated winds w_E, w_N are described in Appendix C, Figure C2 ($w_N = 0$). On the other hand, $\Delta w_E = - w_E$ and $\Delta w_N = - w_N$, so that the system model has no winds.

The filters simulated are the J-Adaptive filter for unmodeled accelerations (with $u_{ii} = (5 \times 10^{-4})^2$, $i = 1, 3$, $Q \equiv 0$), the J-Adaptive filter for C_L and C_D (with $u_{11} = (1 \times 10^{-2})^2$, $u_{22} = (6 \times 10^{-3})^2$, $Q \equiv 0$), and the Extended Kalman filter with Q ($c_2 = 5 \times 10^{-3}$ in Eqn. (7-3)). These parameter values are best engineered values. It should be noted that the J-Adaptive filters are not very sensitive to the choice of U, while the Extended Kalman filter is quite sensitive to the choice of Q. The simulation features radar tracking from nine stations plus on-board accelerations. The radar coverage is indicated in Figure 8.

Position and velocity estimation errors for these filters are shown in Figures 8 and 9. Here again the peaks in the error curves correspond to skips in the reentry trajectory and/or tracking data gaps or low elevation angle radar coverage. The peak around 1000 sec corresponds to both a skip and a data gap.

It is seen that the Extended Kalman filter with Q does not track and tends to diverge. It is not easy to engineer a good Q. Furthermore, this filter has a bad numerical feature in the sequential mode. When Q is added in propagation, the covariance matrix P increases; and when data is processed, P decreases. This causes fluctuations of several orders in magnitude in P, tending to cause ill-conditioning and destroying the the correlations or the geometry of P.

The J-Adaptive filter for C_L and C_D tracks well, except in the regions of the wind gusts (750-950, 1450-1650 sec). Actually, it does not quite recover from the second wind gust. This is because the lift and drag directions span the space of all the model errors with the exception of the winds. As a consequence, this adaptive filter is not adequate in general and needs to be augmented with another variable in the direction orthogonal to lift and drag. It may be noted (see Figure 9) that, prior to the encounter with the first wind gust, the J-Adaptive filter for C_L and C_D tracks extremely well, better than the J-Adaptive filter for unmodeled accelerations. This is because the first adaptive filter has a better prediction model than the second one.

Figures 8 and 9 indicate that the J-Adaptive filter for unmodeled accelerations tracks quite well in the presence of arbitrary model errors, even through the winds. Of course the errors simulated are quite large and this limits the possible tracking accuracy. Tracking accuracy could be improved either by making model errors smaller or giving the filter more tracking data. Toward the end of the trajectory, when multiple station coverage is available, the position and velocity errors almost approach the radar noise level.

How well the J-Adaptive filter for unmodeled accelerations actually tracks these unmodeled accelerations can be seen in Figure 10. Plotted in this figure is the ratio

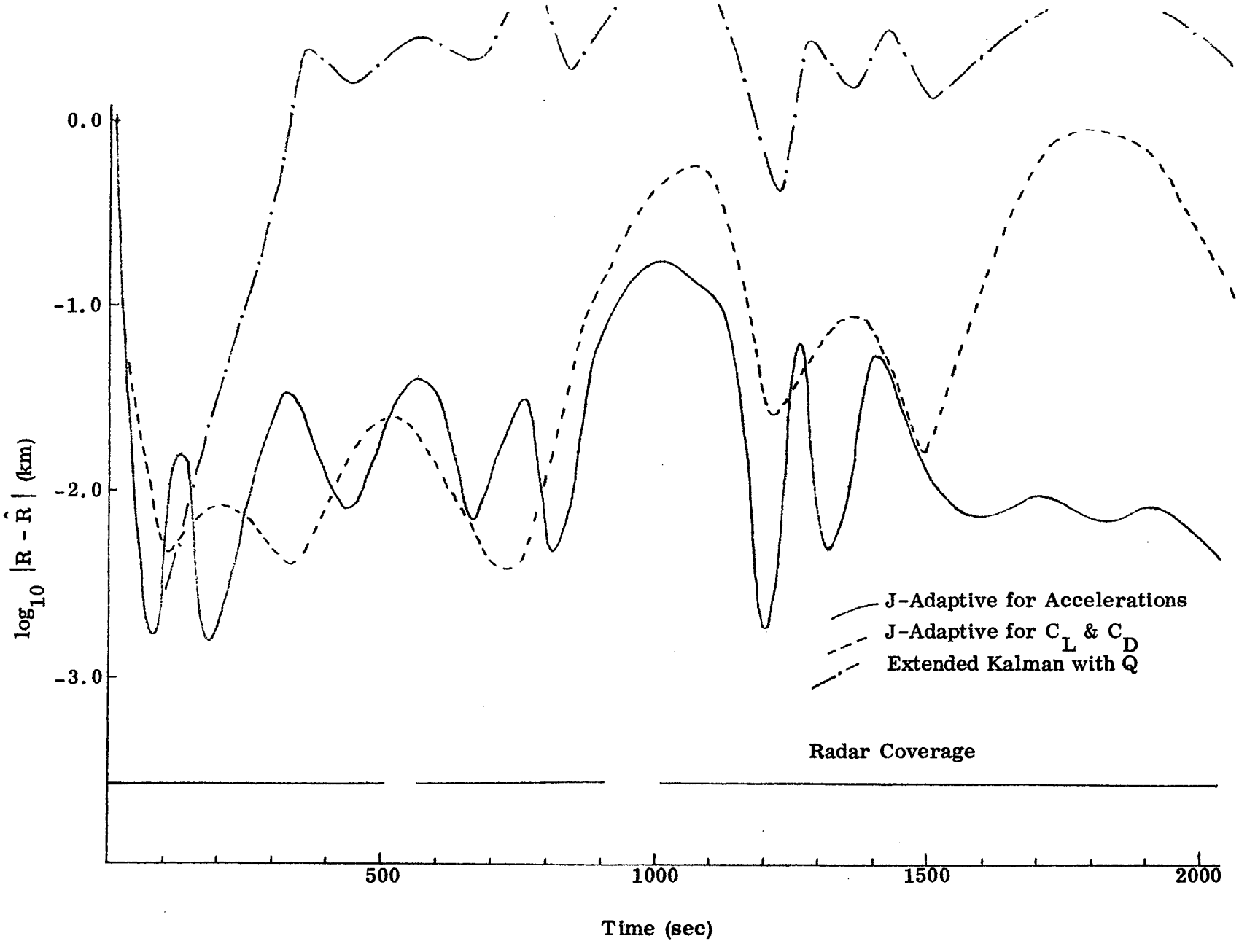

FIGURE 8

Position Estimation Errors

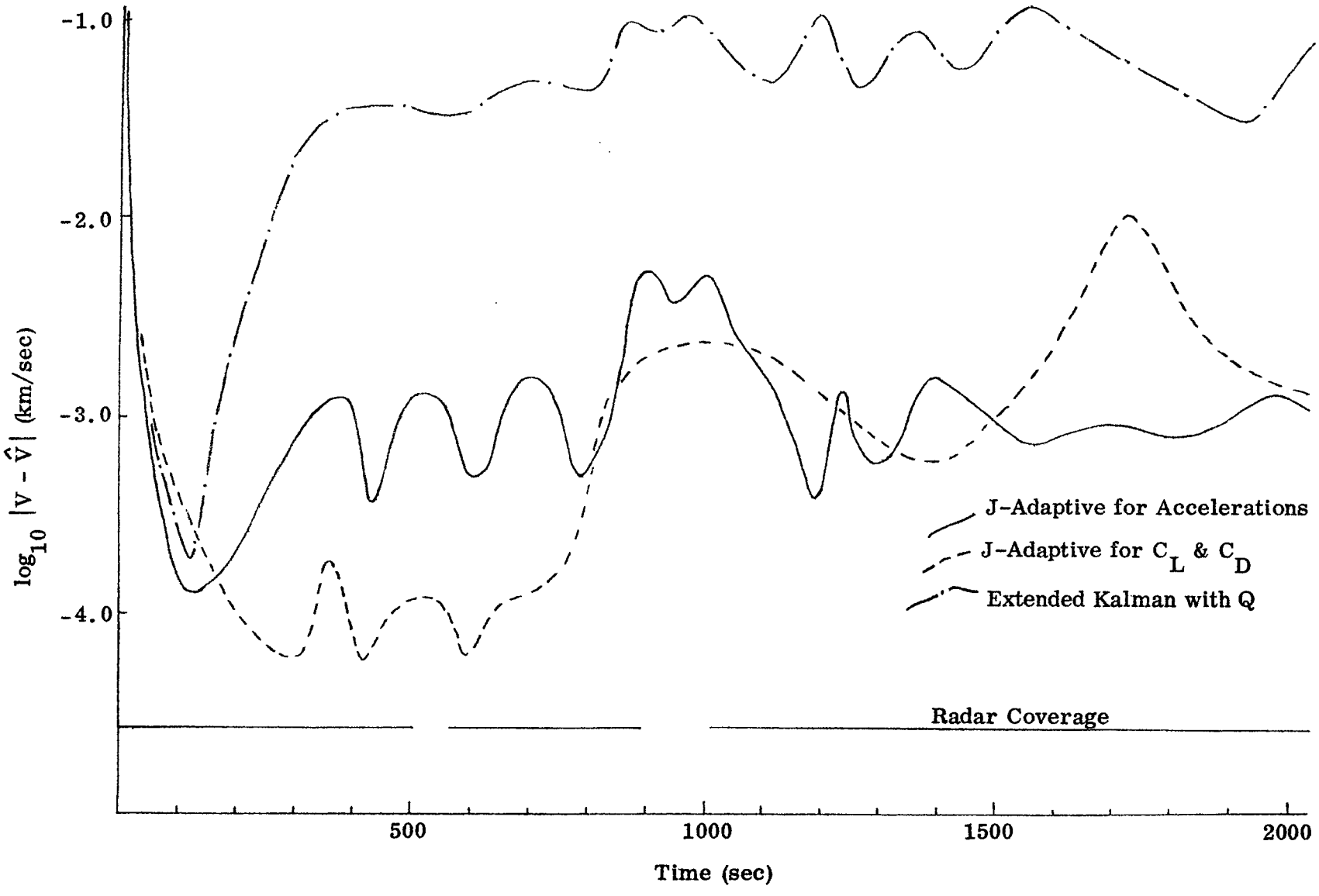

FIGURE 9

Velocity Estimation Errors

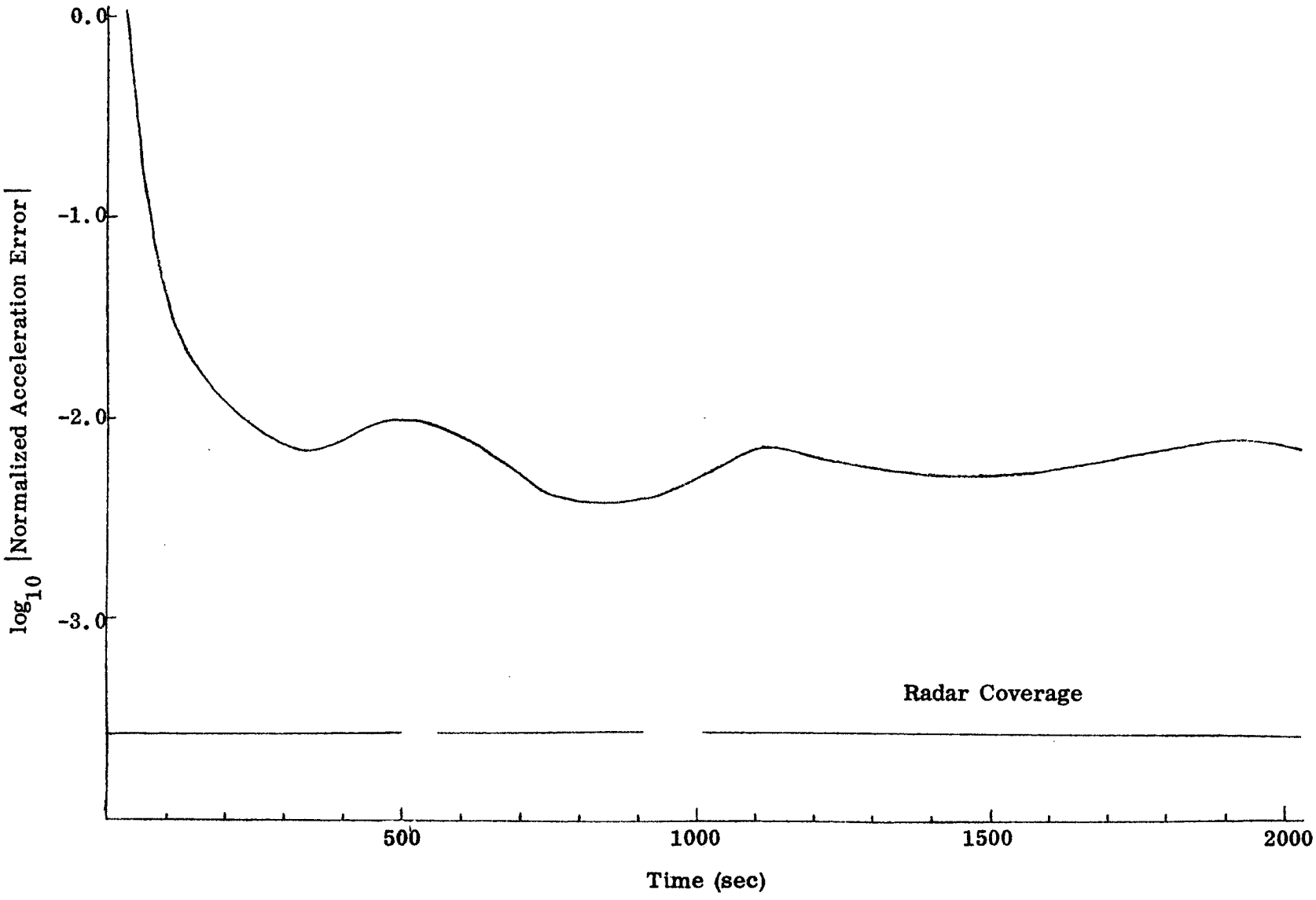

FIGURE 10

Normalized Acceleration Error

$$\frac{|y_a - \hat{a}\ \text{modeled} - \hat{u}\ |}{|y_a - \hat{a}\ \text{modeled}\ |}$$

The denominator in this ratio approximately measures the net acceleration error due to the model errors simulated, while the numerator is the residual acceleration error after using our estimate of the unmodeled acceleration u. It is seen that the J-Adaptive filter identifies 99% of the unmodeled accelerations.

It should be noted that all computations performed in this study were in inertial coordinates. This is not the most convenient system for specifying U in the J-Adaptive filter. Performance of the J-Adaptive filter may further be enhanced by specifying levels of uncertainties in the acceleration vector in other coordinates (e.g. body coordinates).

10.0 CONCLUSIONS AND RECOMMENDATIONS

We believe that the results of this study have several important and practical implications for reentry estimation and for other estimation problems as well.

First, significant nonlinearities indeed exist in the reentry estimation problem. The Iterated Extended Kalman filter appears to offer a practical solution for tracking through nonlinearities without degrading the information content of the data. A practical filter could use this iteration feature when it is appropriate to do so. Other comments concerning estimation in the presence of nonlinearities may be found in Section 9.1.

The J-Adaptive filter concept is sound and shows great promise for practical estimation problems. It can be used to identify models in real time as well as strictly for tracking, as in the unmodeled acceleration mode (Section 7.3). J-Adaptive identification of lift and drag coefficients could perhaps proceed in the presence of arbitrary model errors by the introduction of a third orthogonal variable, provided vehicle mass and atmospheric density errors are not too severe. This concept is clearly applicable to general estimation problems, quite aside from reentry.

On the basis of the results obtained in this study, we recommend that these filter concepts be applied to concrete mission profiles of interest, such as space shuttle reentry. The filters studied have been tested in a realistic environment in the course of study. Their simulation in a concrete mission would serve to further verify these concepts as well as assist in the design of tracking placement and tracking schedules.

We also recommend that the navigation problem be studied in conjunction with guidance and control and attitude determination. Many interactions obviously exist between these problems. The identification of lift and drag coefficients may be required for guidance and control purposes. Guidance accuracies are related to navigation uncertainties. There is an obvious interaction between rotational and translational motion, leading to a coupling between navigation and attitude determination.

The filter concepts developed here (J-Adaptive filter) may be useful in altitude determination, and in the coupling between it and navigation.

In a more research oriented vein, it may be desirable to test certain non-iterative nonlinear filters, such as the Modified Gaussian Second Order filter (see Ref. [1]), in a simulation. Another research area of interest is the adaptive estimation of the J-Adaptive filter covariance matrix U from filter residuals in real time, along the lines of the adaptive filter described in Ref. [1]. This could lead to the elimination of the last engineered parameter in the filter.

11.0 REFERENCES

[1] A. H. Jazwinski, Stochastic Processes and Filtering Theory (book), Academic Press, New York, 1970.

[2] S. Pines and A. H. Jazwinski, "Error Analysis of Space Trajectories," presented at the Fourth IFAC Symposium on Automatic Control in Space, Dubrovnik, Yugoslavia, September, 1971.

[3] W. E. Wagner, "Re-Entry Filtering, Prediction and Smoothing," J. Spacecraft, Vol. 3, No. 9, pp. 1321-1327, September 1966.

[4] R. K. Mehra, "A Comparison of Several Nonlinear Filters for Re-entry Vehicle Tracking," unpublished paper, Systems Control, Inc., Palo Alto, California.

C.2

APPENDIX A - FIGURE OF THE EARTH

The cross section of the oblate earth (see Figure A), in any plane containing the polar axis (z), is an ellipse described by

$$r_p^2 \xi^2 + r_E^2 z^2 = r_p^2 r_E^2 \quad . \tag{A-1}$$

The eccentricity of the earth ellipse is

$$e^2 = 1 - \left(\frac{r_p}{r_E}\right)^2 \quad , \tag{A-2}$$

so that Eqn. (A-1) can be written as

$$\xi^2 + \frac{z^2}{(1-e^2)} = r_E^2 \quad . \tag{A-3}$$

We wish to determine the radius of the earth at some point (ξ_o, z_o). Now

$$r_o^2 = \xi_o^2 + z_o^2 \quad . \tag{A-4}$$

Solving Eqn. (A-3) for ξ_o, we get

$$\xi_o^2 = \frac{r_E^2}{1 + \frac{\tan^2\varphi}{1 - e^2}} \quad . \tag{A-5}$$

Multiplying Eqn. (A-5) by $z_o^2 / \xi_o^2 = \tan^2\varphi$, we get

$$z_o^2 = \frac{r_E^2 \tan^2\varphi}{1 + \frac{\tan^2\varphi}{1-e^2}} \quad , \tag{A-6}$$

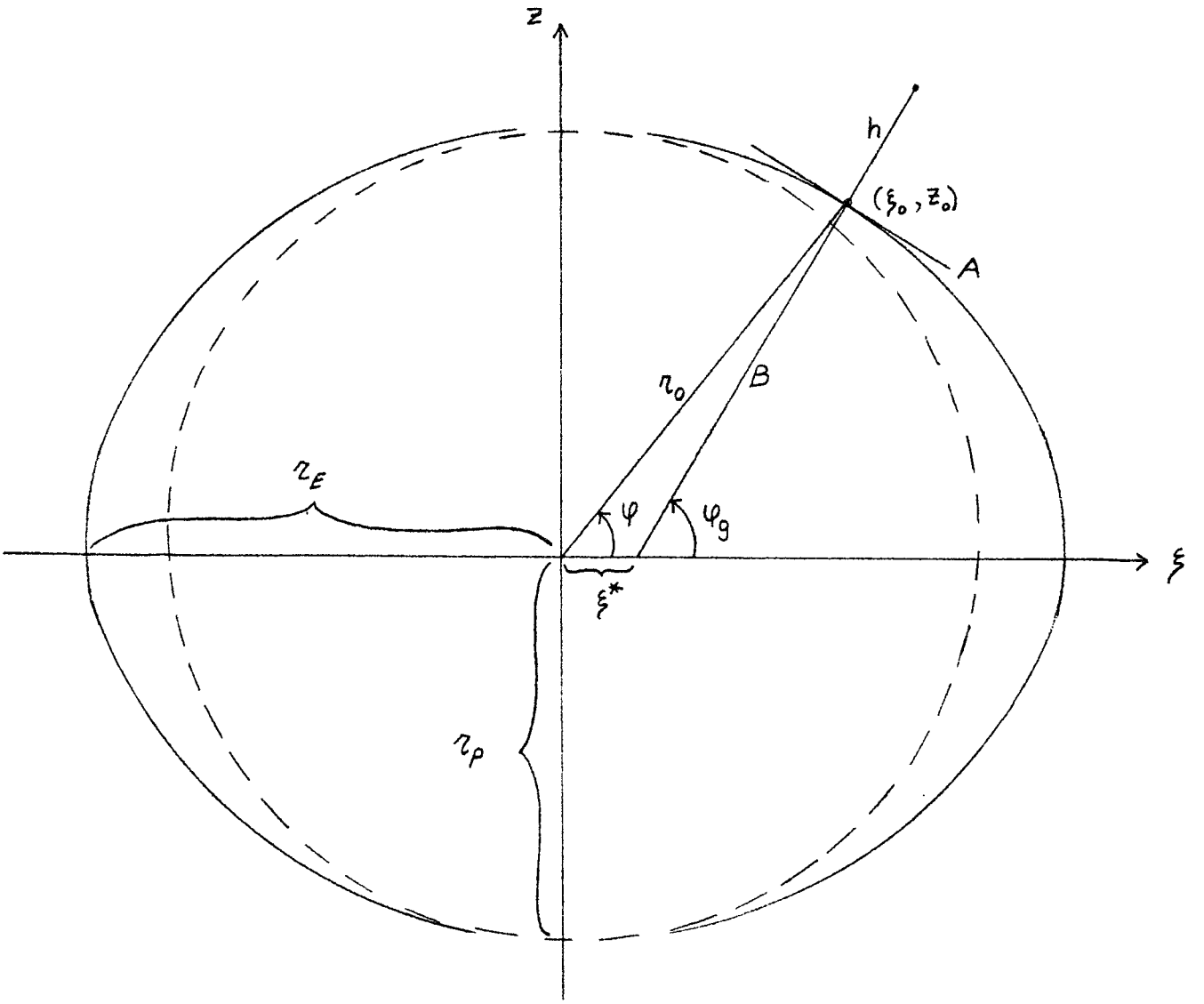

FIGURE A

Figure of the Earth

and then from Eqn. (A-4) we obtain

$$r_o^2 = \frac{r_E^2 (1+\tan^2\varphi)}{1+\dfrac{\tan^2\varphi}{1-e^2}} = \frac{r_E^2}{1+\left(\dfrac{e^2}{1-e^2}\right)\sin^2\varphi} \quad ,$$

so that

$$r_o = r_E\left[1+\left(\frac{e^2}{1-e^2}\right)\sin^2\varphi\right]^{-\frac{1}{2}} = r_E\left[1+\left(\frac{e^2}{1-e^2}\right)\left(\frac{z}{r}\right)^2\right]^{-\frac{1}{2}} \quad . \tag{A-7}$$

We next determine the distance ξ^* (Figure A). The slope of line A, which is tangent to the ellipse, is obtained by differentiating Eqn. (A-3),

$$\left(\frac{dz}{d\xi}\right)_o = -(1-e^2)\,\frac{\xi_o}{z_o} \quad . \tag{A-8}$$

Then the slope of the normal (line B) is

$$\tan\varphi_g = -\frac{1}{\left(\dfrac{dz}{d\xi}\right)_o} = \frac{1}{(1-e^2)}\,\frac{z_o}{\xi_o} \quad . \tag{A-9}$$

It then follows that the equation of line B is

$$z = -\frac{z_o e^2}{1-e^2} + (\tan\varphi_g)\,\xi \quad . \tag{A-10}$$

Evaluating Eqn. (A-10) at $z = 0$ we get

$$\xi^* = \xi e^2 \quad . \tag{A-11}$$

Equations (A-7) and (A-11) are exactly correct only if the vehicle is on the earth surface. At altitude, r_o given by Eqn. (A-7) is not the radius at the sub-vehicle

point. However, at reentry altitudes, the errors in these equations are very small.

Now by definition,

$$\tan \varphi = \frac{z}{\xi} = (1-e^2) \tan \varphi_g \quad , \tag{A-12}$$

where the last equality follows by Eqn. (A-9). This provides us with the relationship between geocentric and geodetic latitudes (exact on the earth's surface).

Equations (A-3) and (A-12) can be solved simultaneously for z and ξ

$$z = \frac{r_E(1-e^2) \sin \varphi_g}{\left(1-e^2 \sin^2 \varphi_g\right)^{\frac{1}{2}}} \quad ,$$

$$\xi = \frac{r_E \cos \varphi_g}{\left(1-e^2 \sin^2 \varphi_g\right)^{\frac{1}{2}}} \quad .$$

Defining

$$a_1 = (1 - e^2 \sin^2 \varphi_g)^{-\frac{1}{2}}$$

$$a_2 = (1 - e^2)\, a_1 \tag{A-13}$$

we get

$$\xi = r_E a_1 \cos \varphi_g \quad ,$$

$$z = r_E\, a_2 \sin \varphi_g \quad . \tag{A-14}$$

At altitude h,

$$\xi = (r_E\, a_1 + h) \cos \varphi_g \quad ,$$

$$z = (r_E\, a_2 + h) \sin \varphi_g \quad . \tag{A-15}$$

APPENDIX B - ATMOSPHERE AND AERODYNAMICS

The air density and speed of sound were obtained from NASA/MSFC, tabulated as a function of altitude. These are reproduced here in TABLE B1. Linear interpolation was used on $\ln \rho$ and c.

The vehicle aerodynamic characteristics were provided by NASA/MSFC and are reproduced here in TABLE B2. These are the estimated trimmed aerodynamic characteristics of the MDAC Delta Orbiter (Dwg. No. 255BJ00029). The vehicle reference area S was given as 5990 ft^2, and vehicle weight as 245703. lbs. Linear interpolation was used on the C_L and C_D tables both in angle of attack α and Mach number M.

Altitude (ft) $h \times 10^{-4}$	Density (slugs/ft^3) $\ln \rho$	Speed of Sound (ft/sec) c
0.0	-8.5497	968.08
6.4997	-8.5497	968.08
9.2070	-9.9009	985.60
9.8550	-11.0226	989.90
12.1330	-11.3280	1025.90
14.3265	-12.2950	1061.90
15.4445	-12.7493	1080.30
16.9277	-13.3185	1082.02
18.6937	-13.9662	1059.85
21.1715	-14.8807	1020.99
22.8226	-15.5359	976.45
24.0154	-16.0476	944.28
24.9131	-16.4579	920.06
25.7791	-16.8751	896.70
25.8999	-16.9350	893.44
26.0199	-16.9949	890.20
26.1649	-17.0677	886.29
28.7548	-18.4552	884.00
34.4373	-21.6258	884.00
40.0000	-24.0498	884.00
50.0000	-24.0498	884.00

TABLE B1

AIR DENSITY AND SPEED OF SOUND

	M = 0 → 0.6			M = 0.9			M = 1.0		
α	C_L	L/D	C_D	C_L	L/D	C_D	C_L	L/D	C_D
5	.150	3.50	.043	.120	2.00	.060	.120	1.80	.067
10	.350	5.25	.067	.280	3.95	.071	.280	3.55	.079
15	.541	4.20	.129	.446	3.09	.144	.439	2.86	.153
20	.710	3.02	.235	.606	2.41	.251	.579	2.29	.253
25	.875	2.28	.384	.735	1.95	.377	.700	1.87	.374
30	.998	1.81	.551	.850	1.59	.535	.815	1.55	.526
35	.982	1.48	.664	.969	1.33	.729	.965	1.30	.742
40	.956	1.22	.784	.995	1.11	.896	1.001	1.10	.910
45	.921	1.01	.912	.968	0.95	1.019	1.005	0.93	1.081
50	.885	0.84	1.054	.935	0.79	1.184	.975	0.78	1.250
55	.847	0.69	1.228	.905	0.66	1.371	.950	0.66	1.439
60	.800	0.55	1.455	.879	0.55	1.598	.925	0.55	1.682

TABLE B2

LIFT AND DRAG COEFFICIENTS

	M = 1.2			M = 1.5			M = 2.0		
α	C_L	$L/_D$	C_D	C_L	$L/_D$	C_D	C_L	$L/_D$	C_D
5	.120	1.60	.075	.105	1.35	.078	.074	1.15	.064
10	.280	3.00	.093	.252	2.80	.090	.193	2.60	.074
15	.446	2.55	.175	.383	2.41	.159	.315	2.31	.136
20	.606	2.10	.289	.521	2.01	.259	.431	1.95	.221
25	.735	1.76	.418	.655	1.70	.385	.545	1.65	.330
30	.850	1.49	.570	.783	1.45	.540	.659	1.39	.474
35	.930	1.27	.732	.954	1.22	.700	.765	1.19	.643
40	.974	1.08	.902	.933	1.05	.889	.865	1.02	.848
45	.993	0.91	1.091	.972	0.90	1.080	.925	0.88	1.051
50	.990	0.78	1.269	.965	0.76	1.270	.934	0.75	1.245
55	.971	0.66	1.480	.962	0.65	1.480	.929	0.64	1.452
60	.946	0.55	1.720	.941	0.55	1.710	.904	0.55	1.644

TABLE B2 (con't)

LIFT AND DRAG COEFFICIENTS

	M = 3.0			M = 4.0 → ∞		
α	C_L	L/D	C_D	C_L	L/D	C_D
5	.049	0.85	.058	.049	0.66	.074
10	.143	2.25	.064	.131	1.40	.094
15	.242	2.23	.109	.219	2.23	.098
20	.342	1.91	.179	.314	1.91	.164
25	.449	1.61	.279	.416	1.61	.258
30	.560	1.39	.403	.525	1.39	.378
35	.680	1.19	.571	.639	1.19	.537
40	.792	1.01	.776	.758	1.02	.743
45	.860	0.88	.977	.830	0.88	.943
50	.882	0.75	1.176	.858	0.75	1.140
55	.867	0.64	1.354	.845	0.64	1.320
60	.836	0.55	1.520	.800	0.55	1.450

TABLE B2 (con't)

LIFT AND DRAG COEFFICIENTS

APPENDIX C - REENTRY TRAJECTORY

The reference trajectory used in this study was obtained from NASA/MSFC. The constants used are

$$\mu = 3.986032 \times 10^{5} \text{ km}^3/\text{sec}^2$$
$$\omega = 7.2921159 \times 10^{-5} \text{ rad/sec}$$
$$e = 0.0$$
$$J_2 = 0.0$$
$$r_E = 6378.1641 \text{ km}$$
$$S = 5.564914 \times 10^{-4} \text{ km}^2$$
$$m = 1.11448 \times 10^{5} \text{ kg}$$

Initial time ($t_o = 0$) is at year = 1970, month = 6, day = 24, hour = 5, min = 55 and sec = 0.0. The initial conditions are

$$x = 2.0147541 \times 10^{3} \text{ km} \qquad \dot{x} = 3.1613972 \text{ km/sec}$$
$$y = -3.3531137 \times 10^{3} \text{ km} \qquad \dot{y} = -5.2614483 \text{ km/sec}$$
$$z = -5.1912063 \times 10^{3} \text{ km} \qquad \dot{z} = 4.7956728 \text{ km/sec}$$

The control functions (angle of attack and roll angle) are shown in Figure C1. The resulting trajectory has the altitude and Mach number profiles as shown in Figure C1. The reentry is essentially from a polar orbit with latitude varying from -53^{o} to 28^{o}.

Some of the simulations performed feature unmodeled winds. The winds used have an east wind component w_E as shown in Figure C2, and $w_N \equiv 0$. This is essentially a crosswind.

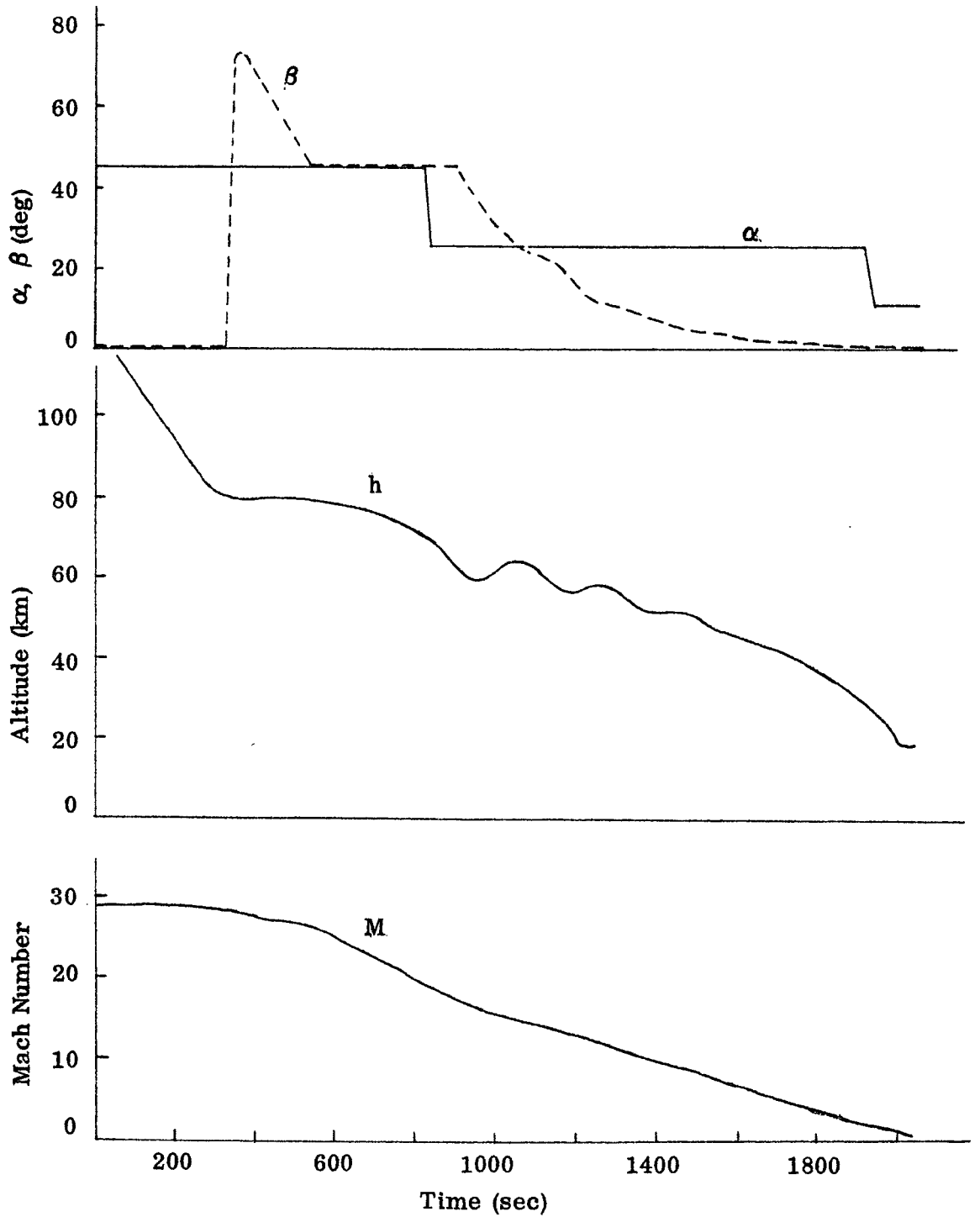

FIGURE C1

REENTRY TRAJECTORY

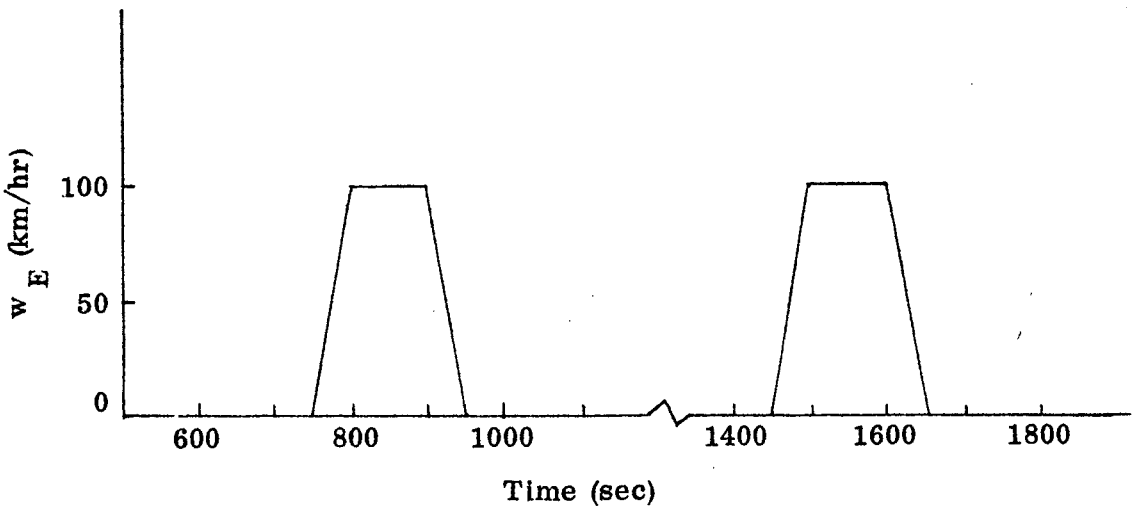

FIGURE C2

EAST WIND COMPONENT